

WE BUILD QUANTUM COMPUTERS

Jan Goetz

www.meetiqm.com

Lecture notes on PHYS-C0254 Quantum Circuits

Short recap from last week

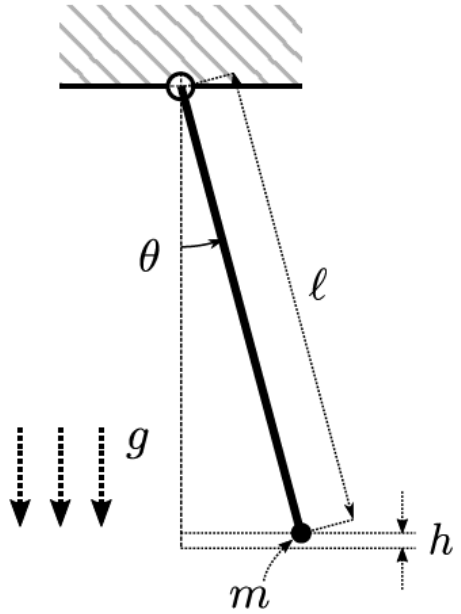


Figure 1: Classical pendulum.

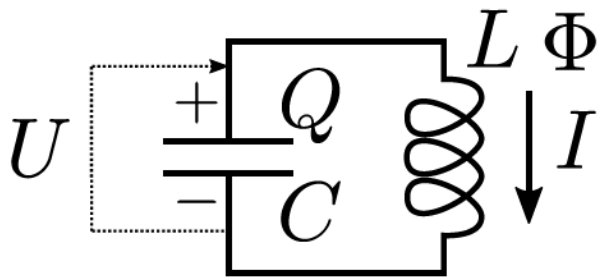
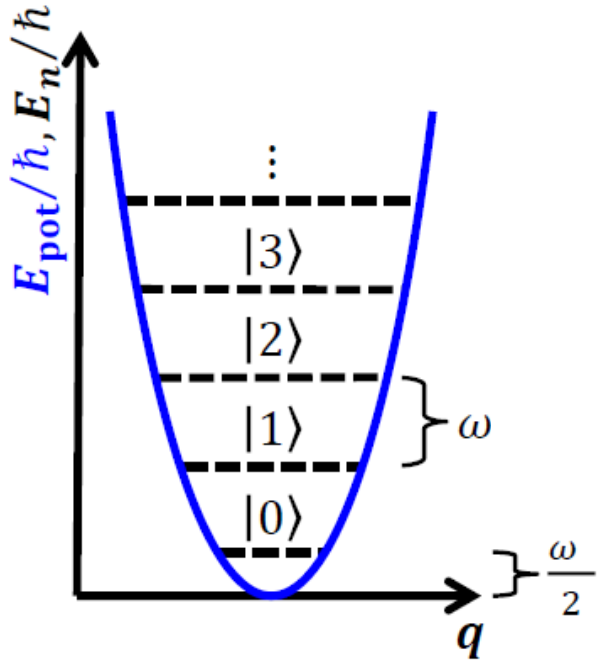


Figure 2: Superconducting LC oscillator.



Key takeaway: Starting from Lagrangian, we can derive the total energy of the system. This is necessary to derive energy quantization.

Key takeaway: Starting from energy considerations, we can derive the eigenfrequency of the system

Key takeaway: The total energy of the system is given by vacuum fluctuations (+1/2) and the number of photons stored at frequency ω

IQM

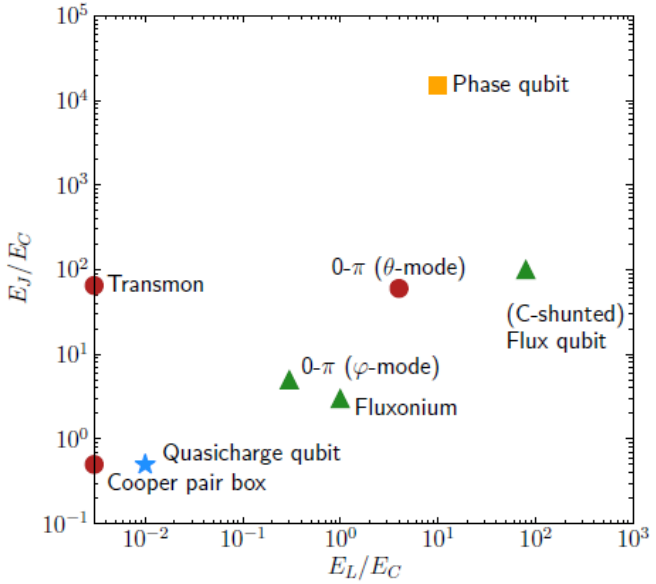
Agenda for lectures 7-12

7. Quantization of electrical networks
    a. Harmonic oscillator: Lagrangian, eigenfrequency
    b. Transfer step: LC oscillator, Legendre transform to Hamiltonian
    d. Quantization of oscillators
8. Superconducting quantum circuits
    a. Qubits: Transmon qubit, Charge qubit, Flux qubit 1st DiVincenzo criteria
    b. Circuit-QED: Rabi model
    c. Rotating Wave approximation: Jaynes-Cummings model
9. Single-qubit operations:
    a. Initialization 2nd DiVincenzo criteria
    b. Control:T1, T2 measurements, Randomized benchmarking 3rd DiVincenzo criteria
    c. Readout 5th DiVincenzo criteria
10. Two-qubit operations: Architectures for 2-qubit gates 4th DiVincenzo criteria
    a. iSWAP
    b. cPhase
    c. cNot
    d. maybe: Google supremacy experiment
11. Quantum algorithms
    a. VQE
    b. Grover search
12. Challenges in quantum computing
    a. Scaling
    b. SW-HW gap
    c. Error-correction

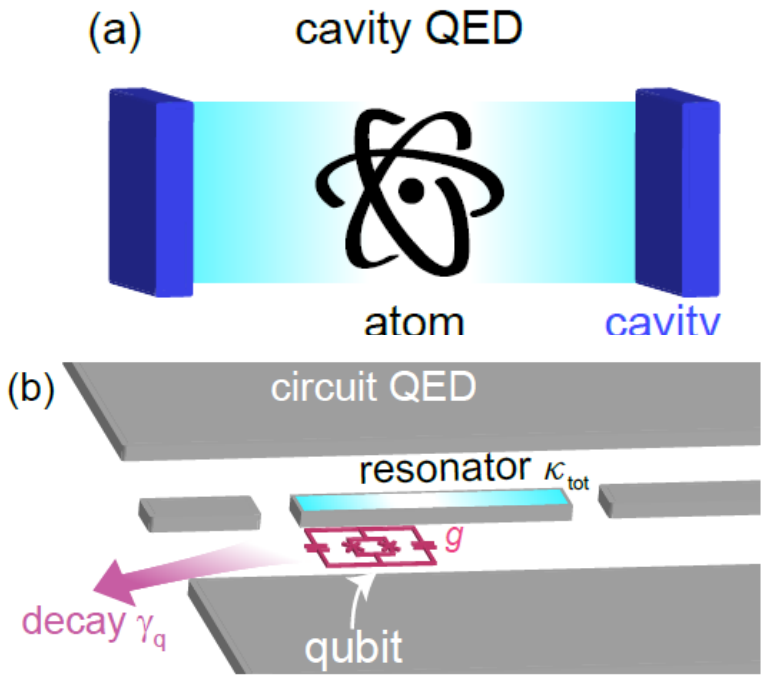
Agenda for today

8. Superconducting quantum circuits
   a. Qubits: Transmon qubit, Charge qubit, Flux qubit 1st DiVincenzo criteria
   b. Circuit-QED: Rabi model
   c. Rotating Wave approximation: Jaynes-Cummings model

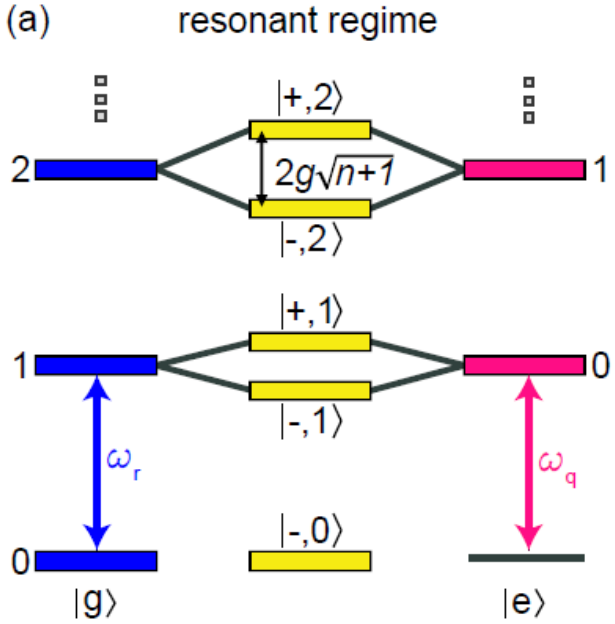
a.



b.

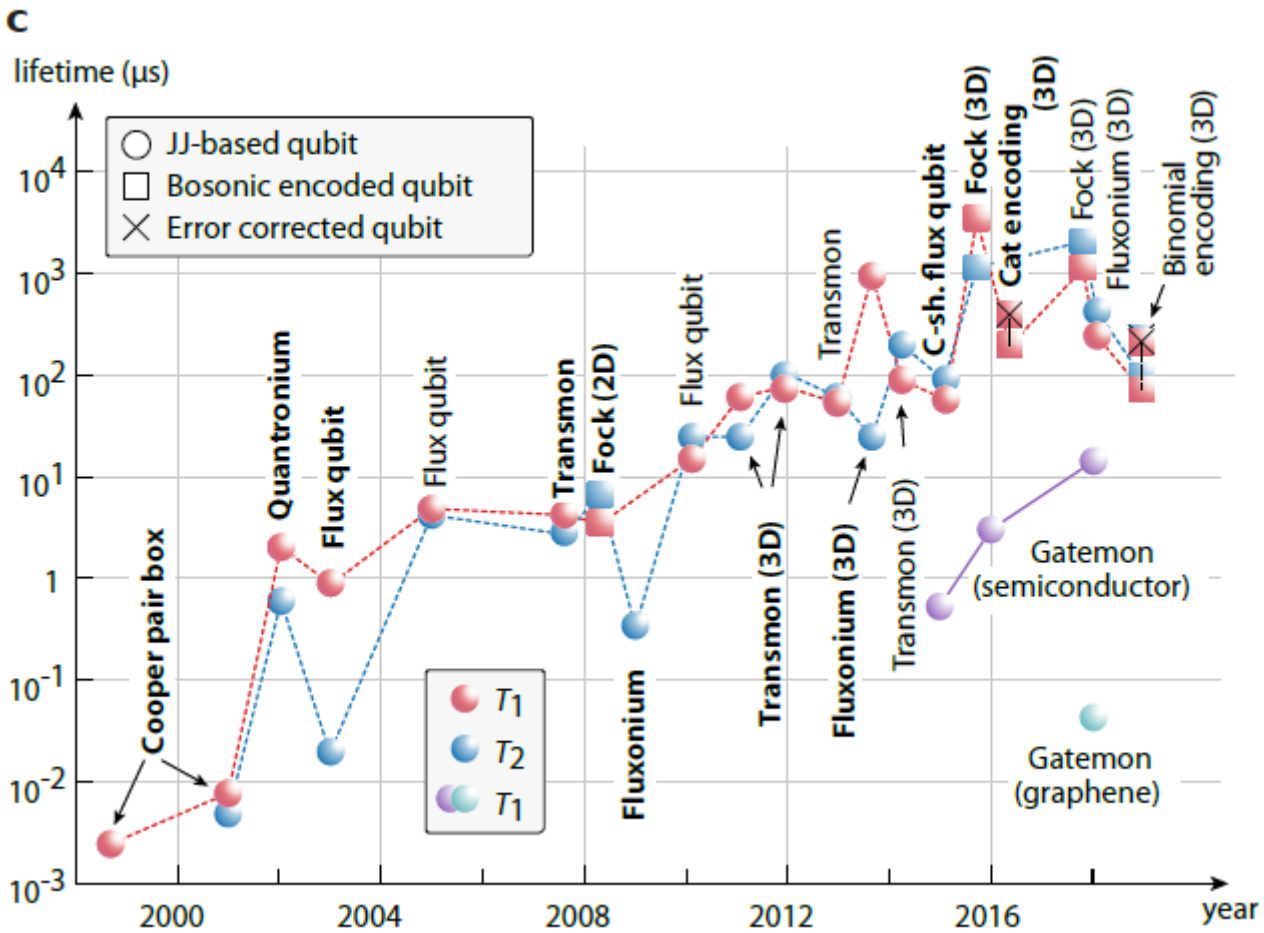


c.



IQM

Short intro: There is a “qubit zoo”



arXiv:1905.13641v3

General approach: Superconducting qubits

- General note: Superconducting circuits have quantized energy levels.
- Josephson junctions are non-linear elements which allow us to make the energy spacing non-equidistant.
- We can create a situation where all but 2 energy levels can be ignored creating effectively a quantum two-level system, i.e., a qubit

Short review: E_J, E_C, E_L

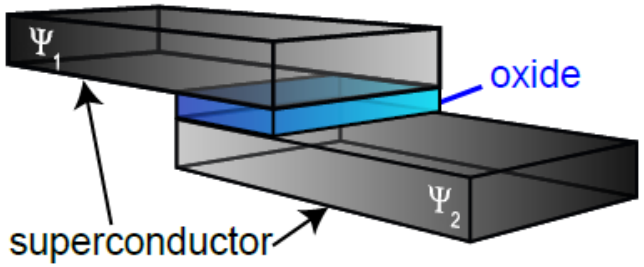
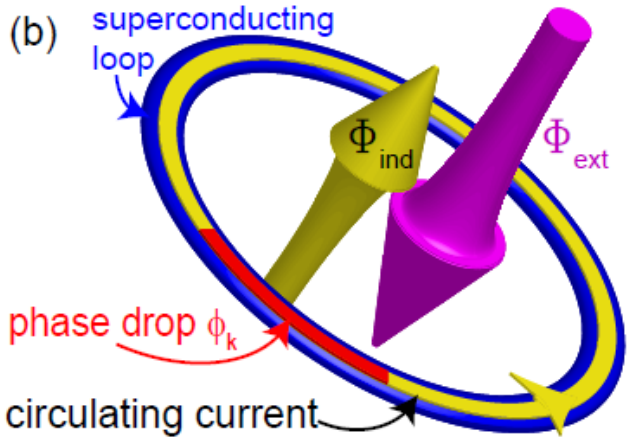


Figure 2.4: Sketch of a Josephson junction.

$$E_J = \frac{\Phi_0 I_c}{2\pi}(1 - \cos\phi_J)$$

$$E_c = e^2/2C$$

$$E_\ell = \frac{1}{2}(L_g + L_k)I_\ell^2$$



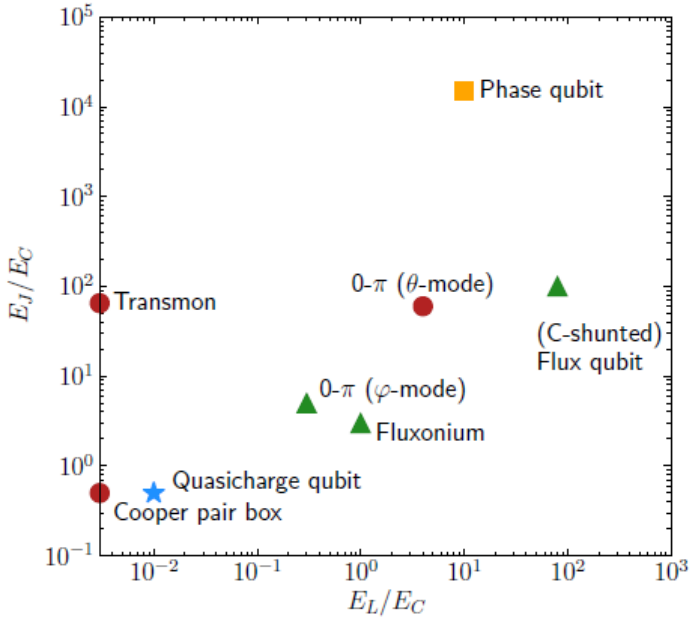


Figure 10. Parameter space of the 'qubit zoo'. The qubits are plotted according to their effective Josephson energy, E_J, and inductive energy, E_L, both normalized by their effective capacitive energy, E_C. The marker indicates the type of qubits, with yellow squares indicating phase qubits, red dots indicating charge qubits, green triangles indicating flux qubits, and a blue star for the quasicharge qubit. Note that the placement of the qubits are only approximate as the effective energies are not definitive. Note that the 0-π qubit is plotted twice, once for each of its modes, where the φ-mode works similar to a fluxonium qubit, while the θ-mode works similarly to the transmon qubit.

arXiv:2103.01225v1

Standard procedure: The charge qubit

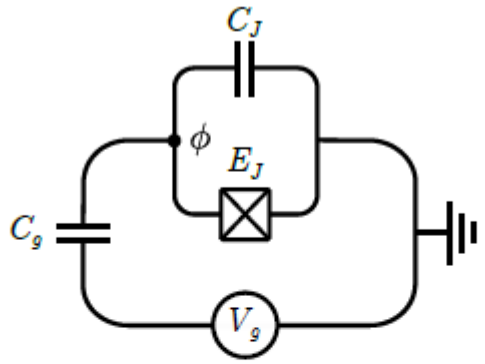


Figure 12. Circuit diagram of the single Cooper pair box, consisting of a Josephson junction, with energy E_J and parasitic capacitance C_J, in series with a capacitor with capacitance C_g. The gate voltage is denoted V_g and the system is connected to the ground in the right corner. There is only one active node, denoted with a dot.

To derive the properties of a charge qubit, we follow the "standard" procedure: Start with a Lagrangian and do a Legendre transform.

In order to write the Lagrangian, we must consider the fixed gate voltage. We model this as an external node with a well-defined flux $\phi_V = V_g t$, meaning $\dot{\phi}_V = V_g$. Setting $\phi^T = (\phi, \phi_V)$ we write the capacitance matrix

$$\boldsymbol{C} = \begin{bmatrix} C_J + C_g & -C_g \\ -C_g & C_g \end{bmatrix}.$$

From this we can write the Lagrangian *L=T-V*

$$\mathcal{L} = \frac{1}{2}\dot{\boldsymbol{\phi}}^T \boldsymbol{C} \dot{\boldsymbol{\phi}} + E_J \cos\phi,$$

details

Standard procedure: The charge qubit

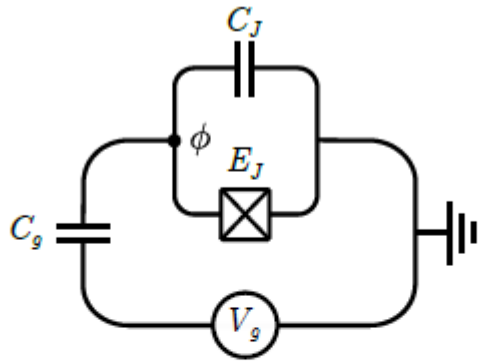


Figure 12. Circuit diagram of the single Cooper pair box, consisting of a Josephson junction, with energy E_J and parasitic capacitance C_J, in series with a capacitor with capacitance C_g. The gate voltage is denoted V_g and the system is connected to the ground in the right corner. There is only one active node, denoted with a dot.

With the Lagrangian, one can obtain the equations of motion from Lagrange's equation

$$\frac{\mathrm{d}}{\mathrm{d}t}\frac{\partial \mathcal{L}}{\partial \dot{\phi}_n} = \frac{\partial \mathcal{L}}{\partial \phi_n}.$$

The Hamiltonian of the circuit can be found by a simple Legendre transformation of the Lagrangian. First we define the conjugate momentum to the node flux by

$$q_n = \frac{\partial \mathcal{L}}{\partial \dot{\phi}_n},$$

which in vector form becomes

$$\boldsymbol{q} = \boldsymbol{C}\dot{\boldsymbol{\phi}}.$$

Note that this requires that the capacitance matrix needs to be invertible.

Standard procedure: The charge qubit

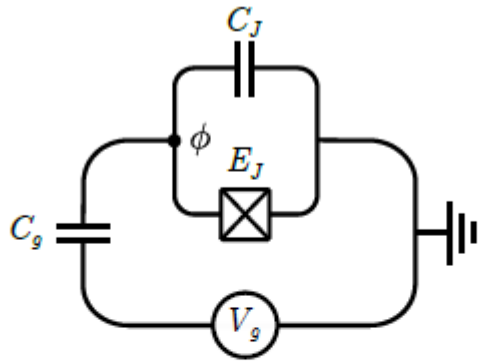


Figure 12. Circuit diagram of the single Cooper pair box, consisting of a Josephson junction, with energy E_J and parasitic capacitance C_J, in series with a capacitor with capacitance C_g. The gate voltage is denoted V_g and the system is connected to the ground in the right corner. There is only one active node, denoted with a dot.

The Hamiltonian can now be expressed in terms of the node charges for the kinetic energy and node fluxes for the potential energy

$$\begin{aligned}\mathcal{H} =& \dot{\boldsymbol{\phi}}^T \boldsymbol{q} - \mathcal{L} \\ =& \frac{1}{2}\boldsymbol{q}^T \boldsymbol{C}^{-1}\boldsymbol{q} + E_{\text{pot}}(\boldsymbol{\phi}),\end{aligned}$$

Solving for $\dot{\phi}$ we do the Legendre transformation and find the Hamiltonian

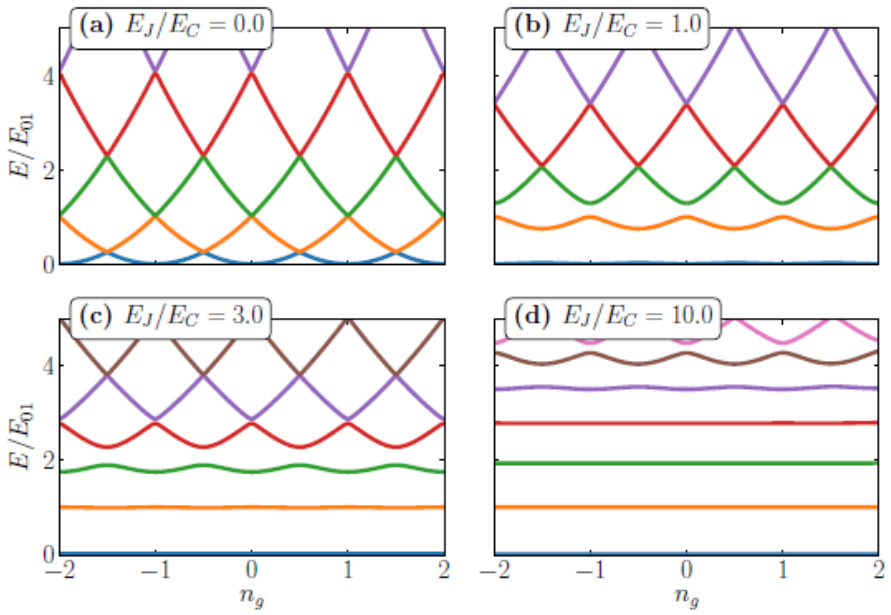
$$\mathcal{H} = \frac{1}{2(C_g + C_J)}(q + C_g V_g)^2 - \frac{C_g V_g^2}{2} - E_J \cos\phi.$$

We now change into conventional notation and define the effective capacitive energy

$$E_C = \frac{e^2}{2(C_g + C_J)},$$

arXiv:2103.01225v1

Standard procedure: The charge qubit



Key takeaway: The quantized energy levels of a charge-biased Josephson junctions can serve as qubit states of a charge qubit

We now quantize the dynamic variables and remove constant terms:

$$\hat{\mathcal{H}} = 4E_C(\hat{n} - n_g)^2 - E_J \cos\hat{\phi},$$

Here, We have further defined the offset charge

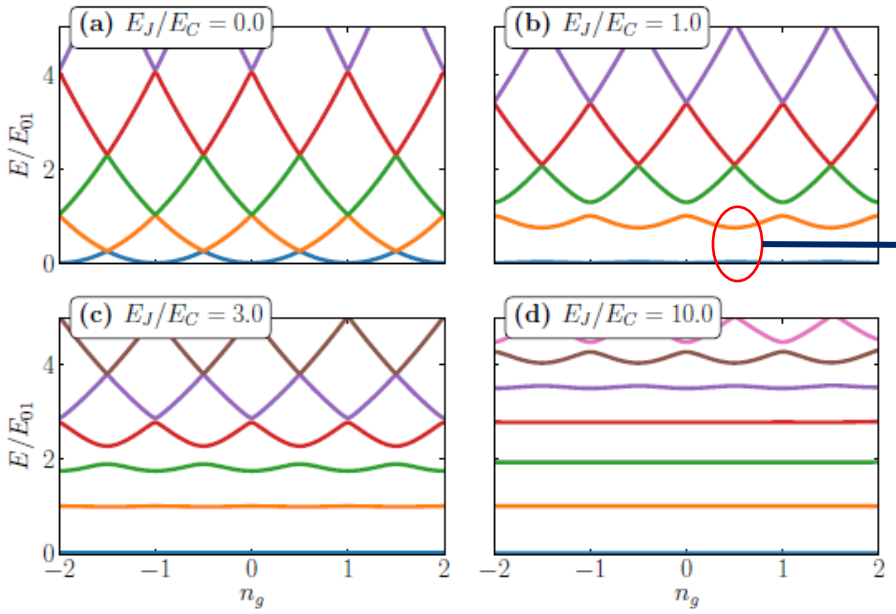
$$n_g = C_g V_g / 2e.$$

We can now discuss certain parameter regimes:

Energy ratio	Effective Hamiltonian	interpretation
$(E_J/E_C = 0)$	$\hat{\mathcal{H}}_C = 4E_C \sum_{n=-\infty}^{\infty} (n - n_g)^2 \lvert n\rangle\langle n\rvert,$	charge states of the capacitor
$E_J/E_C = 1.0$	$\hat{\mathcal{H}} = \hat{\mathcal{H}}_C + \hat{\mathcal{H}}_J,$	Lifted degeneracy, qubit states exist

$$\hat{\mathcal{H}}_J = -\frac{E_J}{2} \sum_{n=-\infty}^{\infty} (\lvert n\rangle\langle n+1\rvert + \lvert n+1\rangle\langle n\rvert).$$

Simplify the model: Qubit description



We can move to a half-integer voltage offset and ignore all the higher-level states. Then, we have a two-level system which is commonly described as

$$\mathcal{H}_\mathrm{q} = \frac{\omega_\mathrm{q}}{2}\hat{\sigma}_\mathrm{z}\,.$$

Here, we have used the Pauli z-operator

$$\sigma_\mathrm{z} = \begin{pmatrix} 1 & 0 \\ 0 & -1 \end{pmatrix}$$

For the qubit eigenbasis

$$\psi_{z+} = \begin{pmatrix} 1 \\ 0 \end{pmatrix}, \qquad \psi_{z-} = \begin{pmatrix} 0 \\ 1 \end{pmatrix}.$$

Key takeaway: The quantized energy levels of a charge-biased Josephson junctions can serve as qubit states of a charge qubit

The birth of superconducting qubits

Published: 29 April 1999

Coherent control of macroscopic quantum states in a single-Cooper-pair box

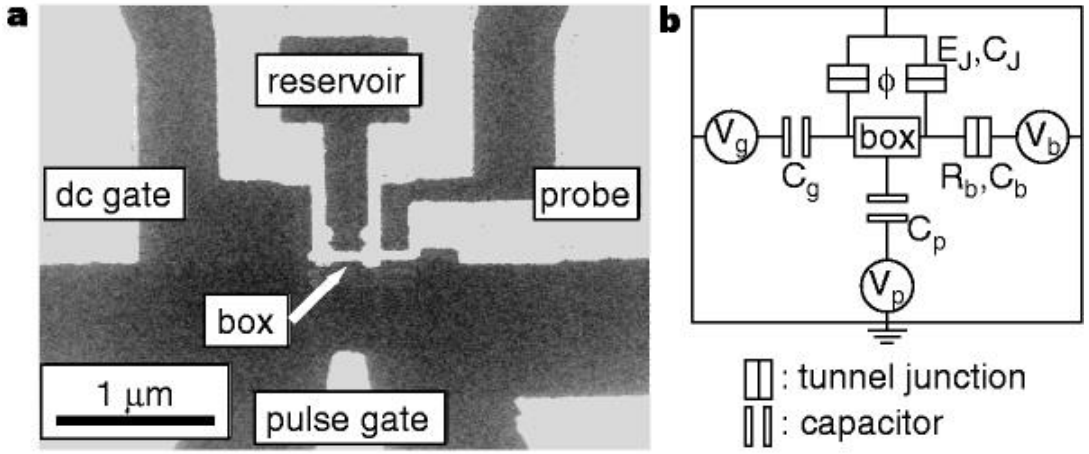
Y. Nakamura ✉, Yu. A. Pashkin & J. S. Tsai

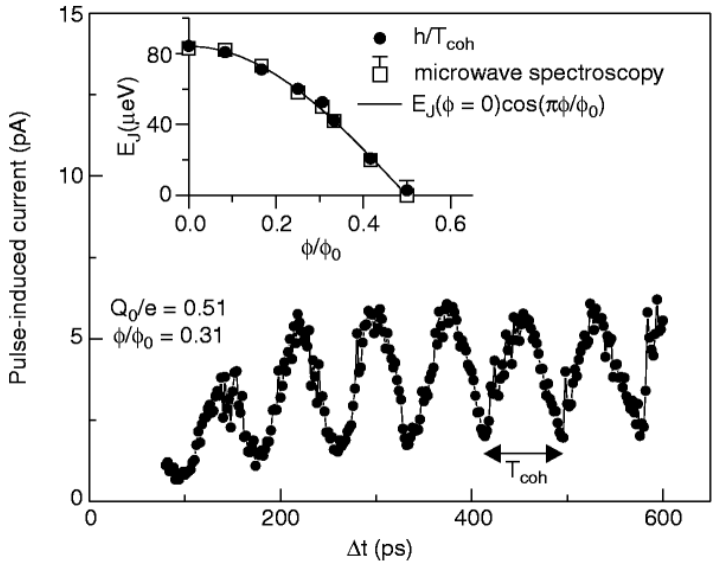
Nature **398**, 786–788(1999) | Cite this article

7509 Accesses | **1858** Citations | **19** Altmetric | Metrics

Abstract

A nanometre-scale superconducting electrode connected to a reservoir via a Josephson junction constitutes an artificial two-level electronic system: a single-Cooper-pair box. The two levels consist of charge states (differing by 2*e*, where *e* is the electronic charge) that are coupled by tunnelling of Cooper pairs through the junction. Although the two-level system is macroscopic, containing a large number of electrons, the two charge states can be coherently superposed[1,2,3,4]. The Cooper-pair box has therefore been suggested[5,6,7] as a candidate for a quantum bit or 'qubit'—the basic component of a quantum computer. Here we report the observation of quantum oscillations in a single-Cooper-pair box. By applying a short voltage pulse via a gate electrode, we can control the coherent quantum state evolution: the pulse modifies the energies of the two charge states non-adiabatically, bringing them into resonance. The resulting state—a superposition of the two charge states—is detected by a tunnelling current through a probe junction. Our results demonstrate electrical coherent control of a qubit in a solid-state electronic device.





https://arxiv.org/abs/cond-mat/9904003

The two directions to approach a transmon qubit:

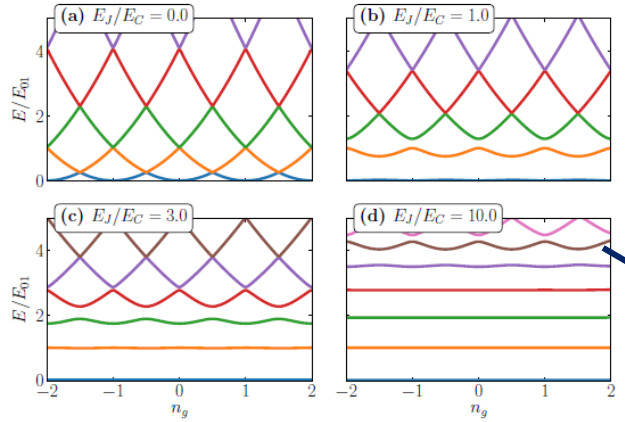
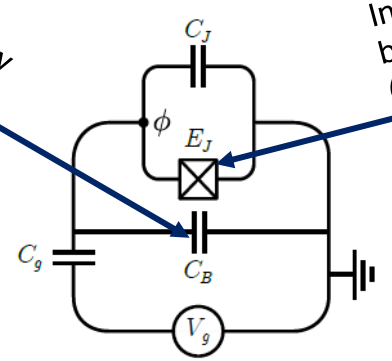


Figure 13. The energies of the lowest lying states of the single Cooper pair box/transmon qubit as a function of the bias charge n_g. The difference between the two lowest bands are approximately equal to E_J at the avoided crossing.

Reduce charge dispersion by introducing a shunt capacitor

Increase anharmonicity by non-linear inductor (Josephson junction)



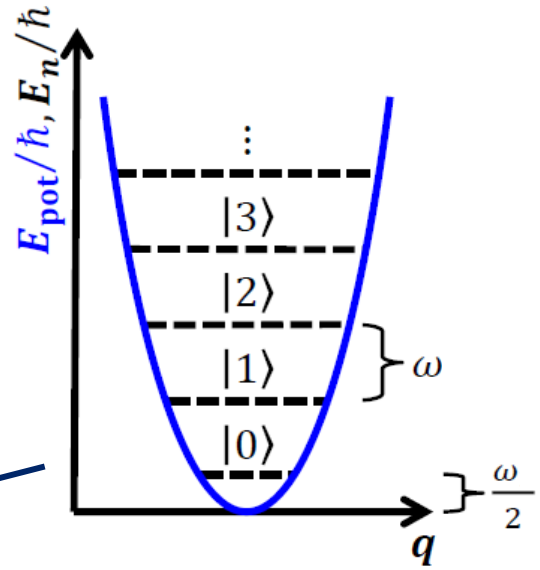
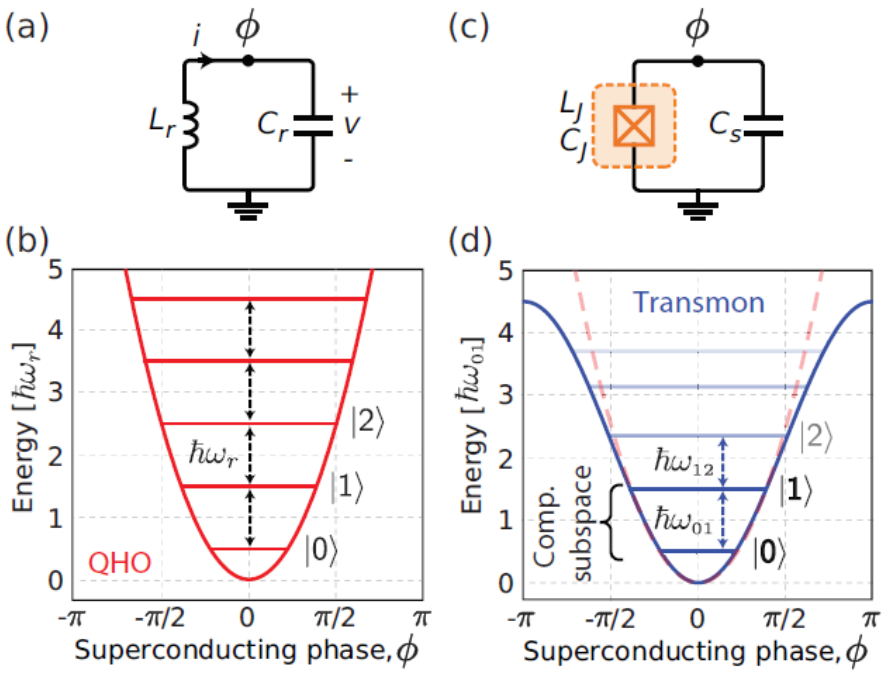


Figure 14. Circuit diagram of the transmon qubit, consisting of a Josephson junction, with energy E_J and parasitic capacitance C_J, in series with a capacitor with capacitance C_g. The system is shunted by a large capacitance, C_B. The gate voltage is denoted V_g and the system is connected to the ground in the right corner. There is only one active node.

arXiv:2103.01225v1

Anharmonic oscillator: The transmon qubit



We have learned that an LC oscillator has equidistant level spacing

$$H = \hbar\omega_r \left(a^\dagger a + \frac{1}{2} \right)$$

To introduce non-equidistant level spacing (qubits), we use a non-linear inductor (Josephson junction)

$$L_\mathrm{J} = \frac{\Phi_0}{2\pi I_\mathrm{c} \cos\phi_\mathrm{J}} = L_\mathrm{c} \frac{1}{\cos\phi_\mathrm{J}}$$

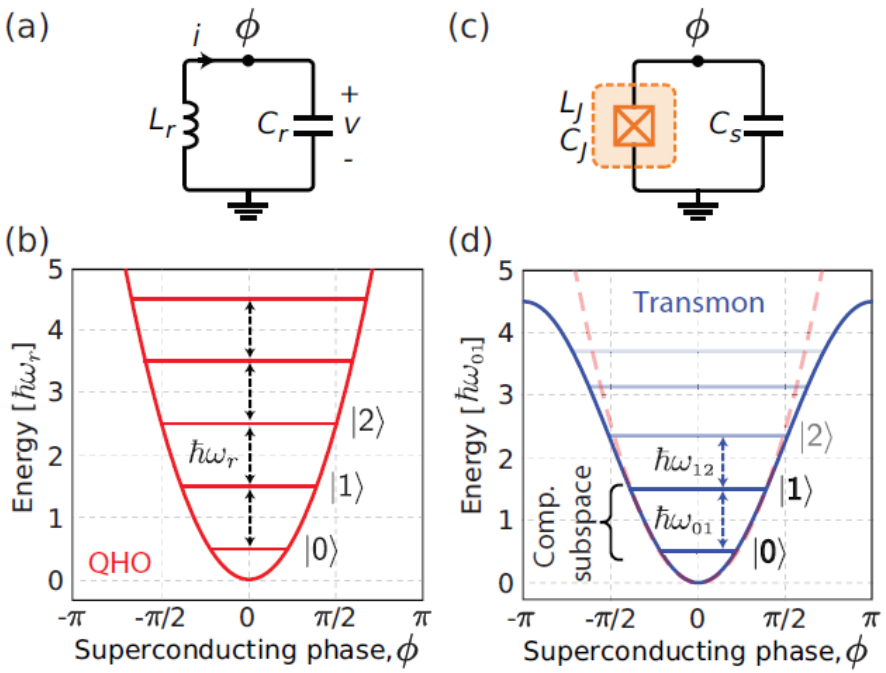
The Hamiltonian of a capacitively shunted Josephson junction has two components

$$\hat{H}_\mathrm{tr} = 4E_c\hat{n}^2 - E_J \cos\hat{\phi},$$

Two parameters, we have to get rid of one …

https://qiskit.org/textbook/ch-quantum-hardware/transmon-physics.html

Anharmonic oscillator: The transmon qubit



Now we can approach the quantization similarly to the quantum harmonic oscillator, where we define the creation and annihilation operators

$$\hat{n} = in_{zpf}(\hat{c} + \hat{c}^\dagger) \quad \text{and} \quad \hat{\phi} = \phi_{zpf}(\hat{c} - \hat{c}^\dagger),$$

Here, $\hat{c}$ denotes the transmon annihilation operator and distinguish it from the evenly-spaced energy modes of $\hat{a}$.

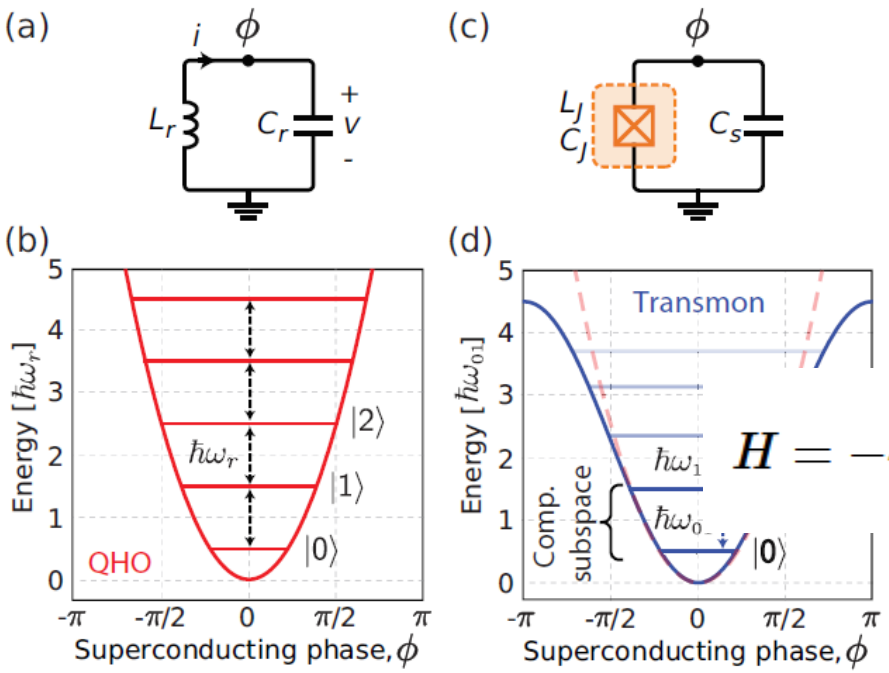
$$\hat{c} = \sum_j \sqrt{j+1}|j\rangle\langle j+1|$$

The prefactors describe vacuum fluctuations (zero point fluctuations, zpf):

$$n_{\text{zpf}} = \left(\frac{E_J}{32E_c}\right)^{1/4} \quad \text{and} \quad \phi_{\text{zpf}} = \left(\frac{2E_c}{E_J}\right)^{1/4},$$

https://qiskit.org/textbook/ch-quantum-hardware/transmon-physics.html

Anharmonic oscillator: The transmon qubit



To assume $\phi \ll 1$, we chose $C_s \gg C_J$ and Taylor expand the E_J term:

$$E_J \cos(\phi) = \frac{1}{2} E_J \phi^2 - \frac{1}{24} E_J \phi^4 + \mathcal{O}(\phi^6).$$

In the $\hat{c}$ basis the complete Hamiltonian therefore reads

$$H = -4E_c n_{zpf}^2 (\hat{c} + \hat{c}^\dagger)^2 - E_J \left(1 - \frac{1}{2}\phi_{zpf}^2 (\hat{c} - \hat{c}^\dagger)^2 + \frac{1}{24}\phi_{zpf}^4 (\hat{c} - \hat{c}^\dagger)^4 + \ldots\right)$$

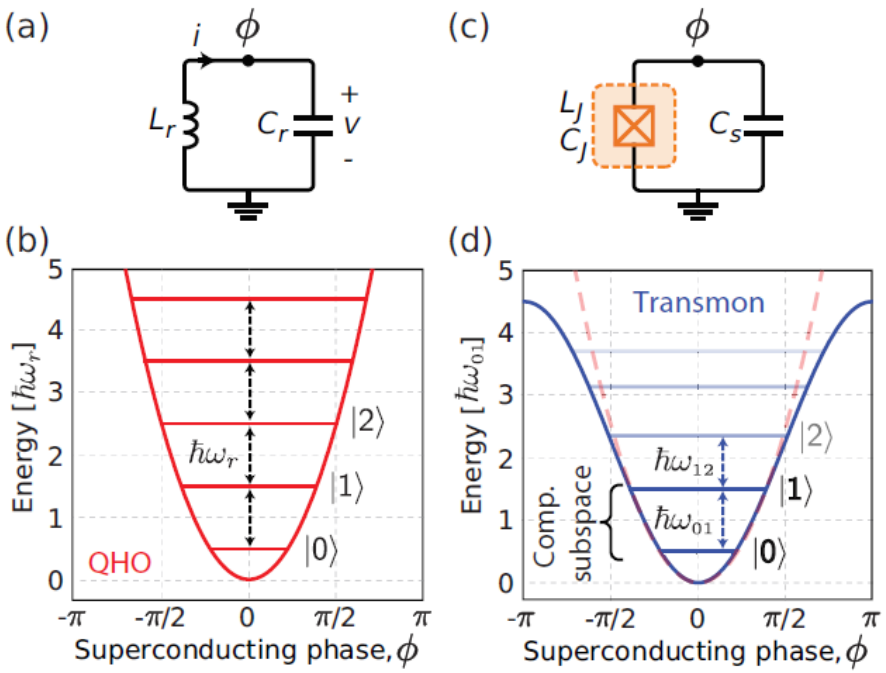
$$\approx \sqrt{8E_c E_J}\left(\hat{c}^\dagger \hat{c} + \frac{1}{2}\right) - E_J - \frac{E_c}{12}(\hat{c}^\dagger - \hat{c})^4,$$

We now use the following relations

$$\hbar\,\omega_0 = \sqrt{8E_c E_J} \qquad \delta = -E_c$$

https://qiskit.org/textbook/ch-quantum-hardware/transmon-physics.html

Anharmonic oscillator: The transmon qubit



Expanding the terms of the transmon operator and dropping the fast-rotating terms (i.e. those with an uneven number of $\hat{c}$ and $\hat{c}^\dagger$), neglecting constants yields

$$\hat{H}_{\text{tr}} = \omega_0 \hat{c}^\dagger \hat{c} + \frac{\delta}{2}\, \hat{c}^\dagger \hat{c}^\dagger \hat{c}\, \hat{c}$$

This is the Hamiltonian of a (non-linear) Duffing Hamiltonian. The energy levels of the system are calculated as

$$\omega_j = \left(\omega - \frac{\delta}{2}\right) j + \frac{\delta}{2} j^2 \qquad \omega \equiv \omega_0 + \delta,$$

Key takeaway: The transmon qubit is actually a non-linear oscillator and we use the two lowest eigenstates as qubit states. They correspond to having 0 or 1 excitations stored in the system

https://qiskit.org/textbook/ch-quantum-hardware/transmon-physics.html

Frequency control: The split transmon qubit

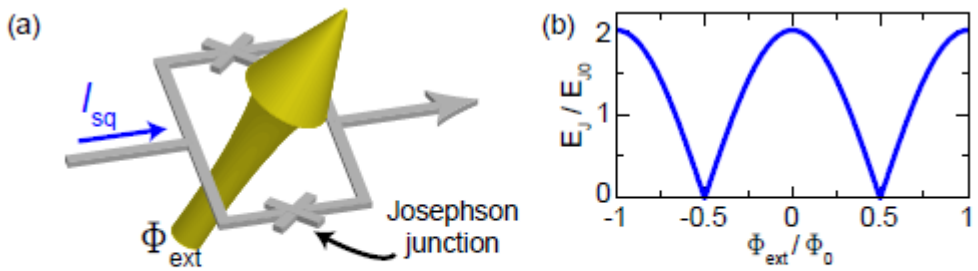
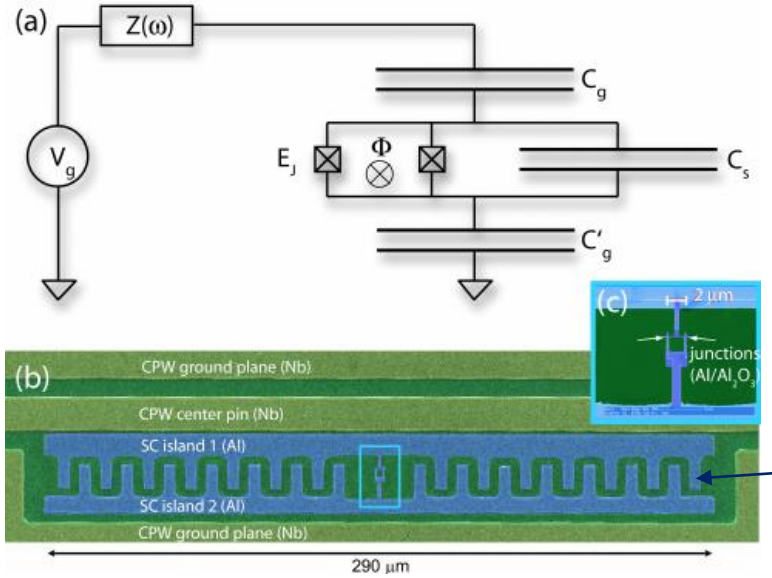


Figure 2.5: **(a)** Sketch of a DC SQUID, consisting of a superconducting loop intersected by two Josephson junctions. The maximum SQUID current I_c depends on the external magnetic flux Φ_ℓ threading the loop. For vanishing screening parameter β_ℓ, we have $\Phi_\ell \simeq \Phi_{ext}$. **(b)** Modulation of the Josephson energy plotted versus external magnetic flux for a negligible screening parameter β_ℓ.

Choosing the two lowest eigenstates as qubit states, allows us to treat the transmon as a qubit with Hamiltonian

$$\mathcal{H}_q = \frac{\omega_q}{2}\hat{\sigma}_z \,.$$

Frequency tunability can be created by replacing the single junction with a split junction, i.e., a DC SQUID



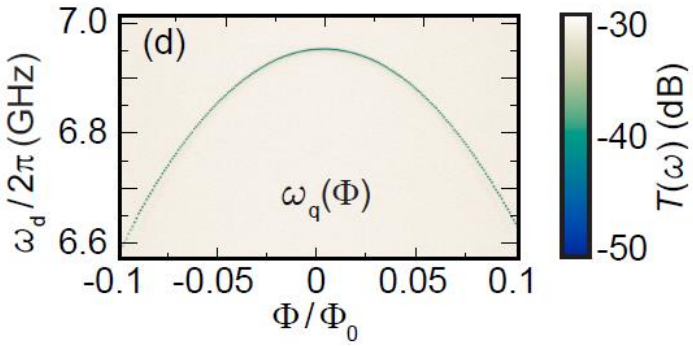


VNA

DUT

$$\omega_q \approx \sqrt{8E_c E_{J0}\left|\cos\left(\pi f_{ext}\right)\right|}$$

Φ / Φ_0



IQM https://mediatum.ub.tum.de/1326240

Closing the loop: The flux qubit

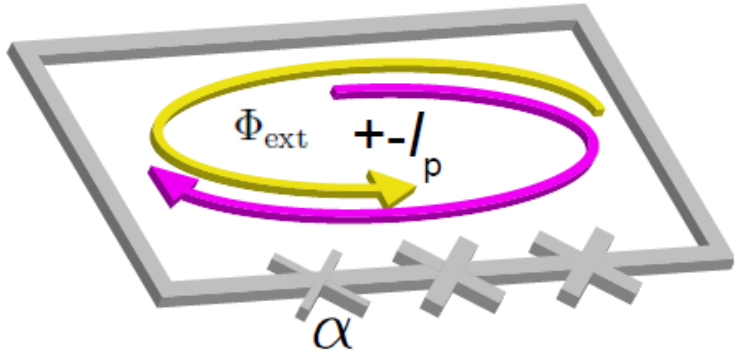


Figure 2.7: Sketch of a three junction flux qubit and the superposition of current states.

In contrast to the charge- and the transmon qubit, the flux qubit operates in the regime $E_{J0} \gg E_c$ such that magnetic flux is the good quantum variable.

The most common implementation is a closed superconducting loop intersected by three Josephson junctions. One junction has a reduced Josephson energy by a factor $0.5 < \alpha < 1$. This yields the potential

$$U_q = E_{J0}\left[2 + \alpha - \cos(\phi_1) - \cos(\phi_2) - \alpha\cos\left(\phi_{ext} + \phi_1 - \phi_2\right)\right]$$

Here, $\phi_{ext} = 2\pi\Phi_{ext}/\Phi_0$ is the reduced magnetic flux threading the qubit loop and ϕ_1, ϕ_2 are the phase differences across the two identical junctions. The third phase difference is eliminated due to the boundary condition imposed by flux quantization.

Flux quantization is guaranteed by a persistent circulating current

$$I_p = \pm I_c\sqrt{1-(2\alpha)^{-2}}$$

IQM https://mediatum.ub.tum.de/1326240

Closing the loop: The flux qubit

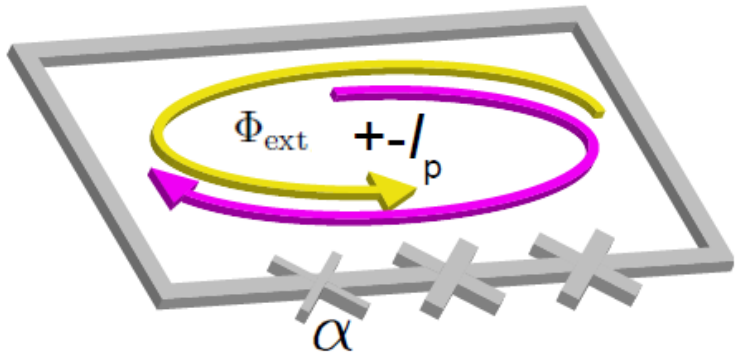
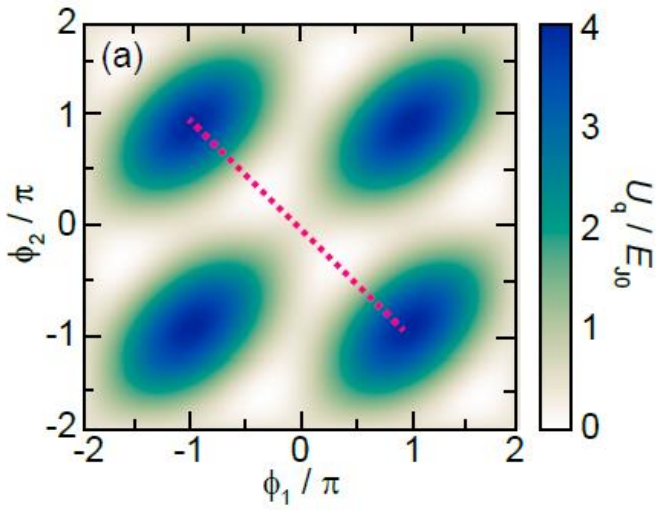


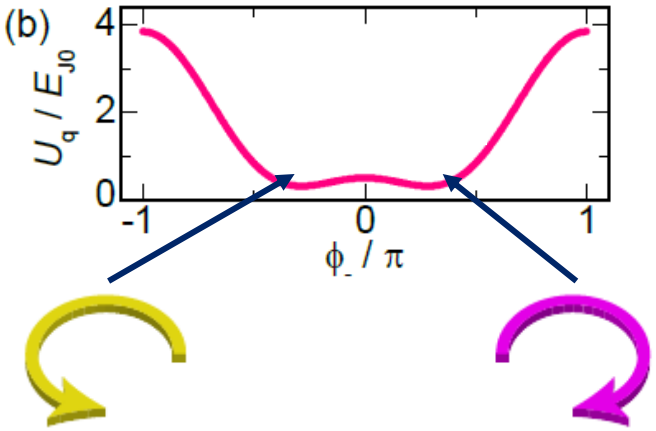
Figure 2.7: Sketch of a three junction flux qubit and the superposition of current states.

The two degrees of freedom result in a two-dimensional potential. For $\phi_{ext} = \pi$, the potential is symmetric and periodic.



Because the two larger junctions are identical, we can only move along the line $\phi_2 = -\phi_1$

The potential along this line has the form of a double well, where the minima correspond to circulating currents in opposite directions.



Closing the loop: The flux qubit

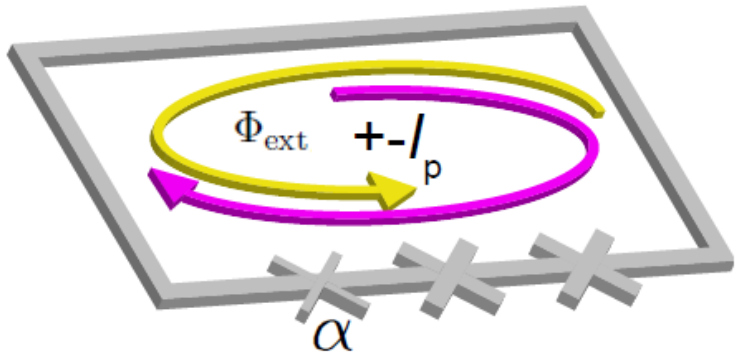
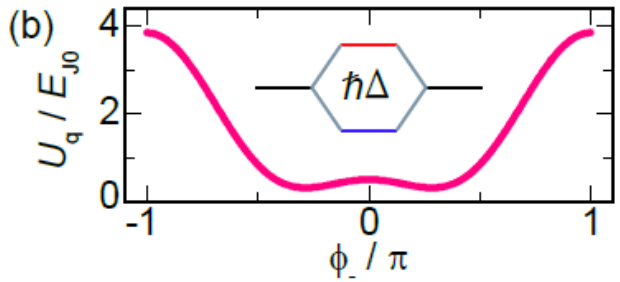


Figure 2.7: Sketch of a three junction flux qubit and the superposition of current states.

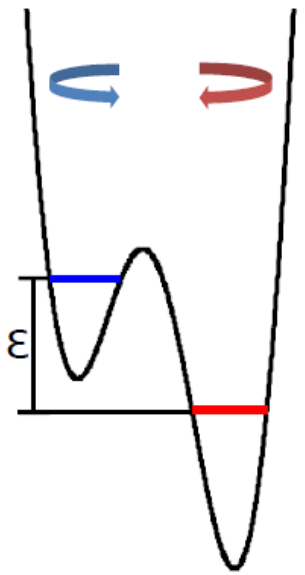
Because the potential barrier has a finite height, there is a certain tunneling probability Δ between the wells.



The tunnel coupling lifts the energy degeneracy between the states, resulting in a level splitting. The resulting two energy levels can be used as two qubit states.

A change in magnetic flux bias tilts the potential leading to an additional energy ε.

$$\mathcal{H}_q = \frac{\hbar\Delta}{2}\hat{\sigma}_x + \frac{\hbar\varepsilon}{2}\hat{\sigma}_z = \frac{\hbar}{2}\begin{pmatrix} \varepsilon & \Delta \\ \Delta & -\varepsilon \end{pmatrix}$$



Closing the loop: The flux qubit

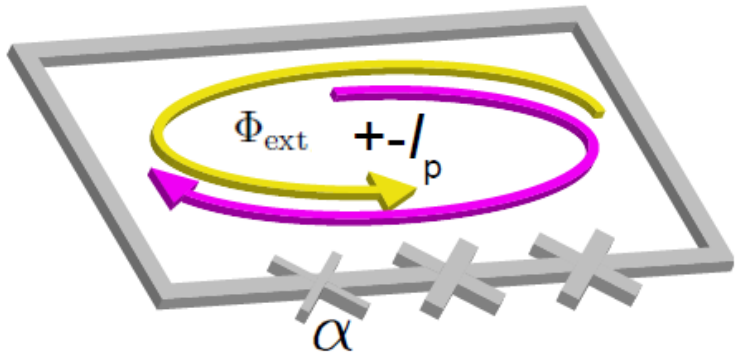


Figure 2.7: Sketch of a three junction flux qubit and the superpo-
sition of

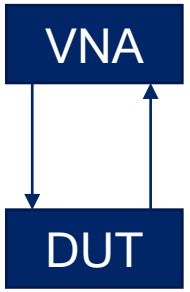
To describe the system with the well-known formalism for quantum two-level systems, we diagonalize the system Hamiltonian to transform into the qubit eigenbasis

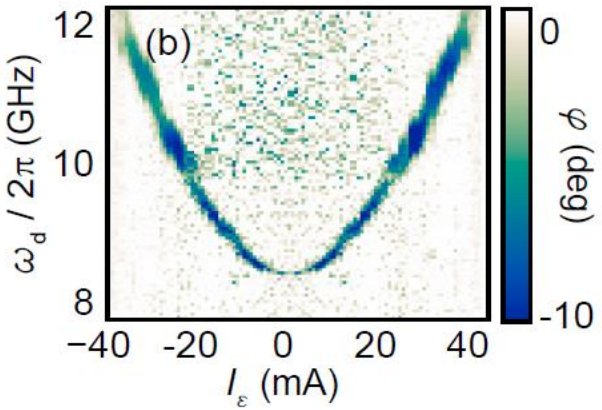
$$\mathcal{H}_q = \frac{\omega_q}{2}\hat{\sigma}_z .$$

Here, the qubit transition frequency is given as

$$\omega_q = \sqrt{\Delta^2 + \varepsilon^2}.$$

Key takeaway: The flux qubit is a closed loop with 3 JJs where the circulating currents provide energy eigenstates that can be treated as a quantum 2-level system.





Φ_{ext}

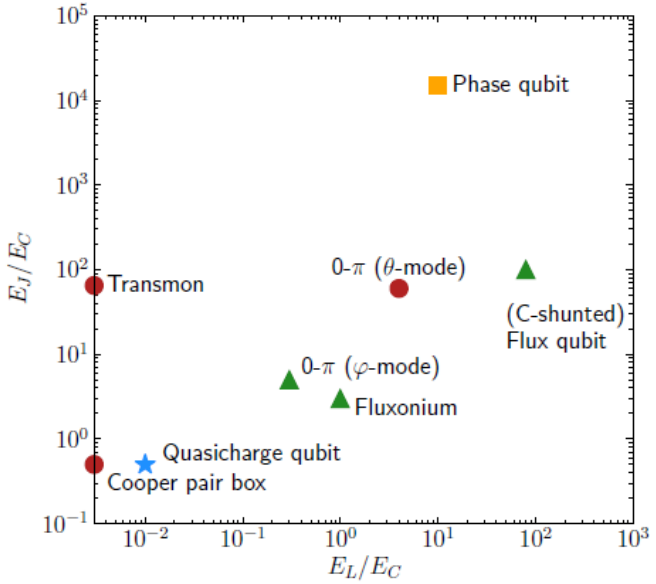
General approach: Superconducting qubits

- General note: Superconducting circuits have quantized energy levels.
- Josephson junctions are non-linear elements which allow us to make the energy spacing non-equidistant.
- We can create a situation where all but 2 energy levels can be ignored creating effectively a quantum two-level system, i.e., a qubit.

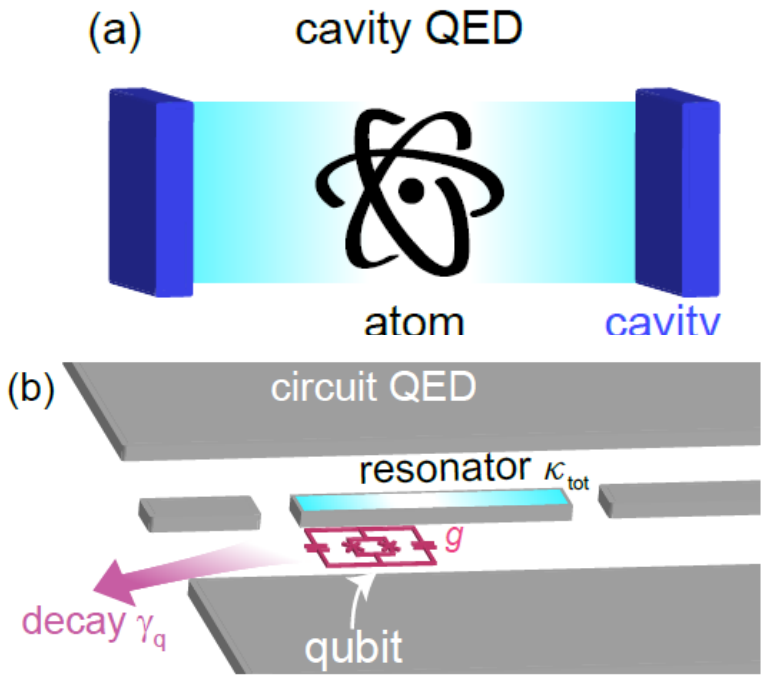
Agenda for today

8. Superconducting quantum circuits
   a. Qubits: Transmon qubit, Charge qubit, Flux qubit 1st DiVincenzo criteria
   b. Circuit-QED: Rabi model
   c. Rotating Wave approximation: Jaynes-Cummings model

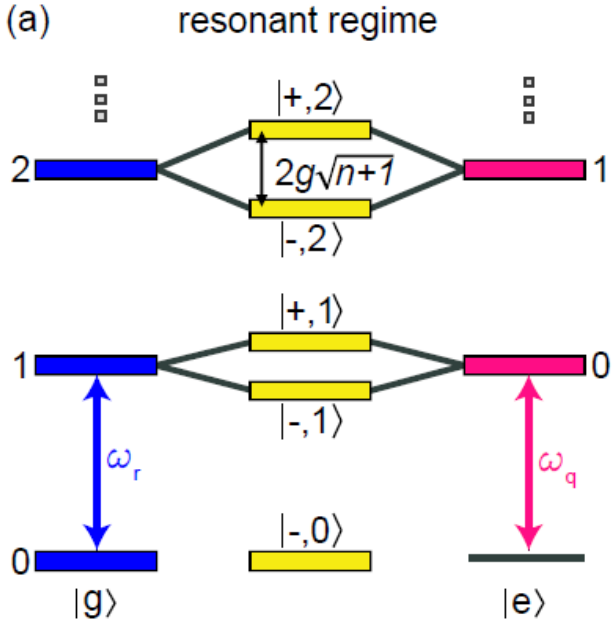
a.



b.



c.



IQM

General note: Circuit QED

- Qubits can be seen as artificial atoms and resonators as microwave light.
- When we bring them close to each other we create “light-matter” coupling that is treated in the same way as quantum optics.
- Superconducting circuits allow on-chip study of quantum optics in regimes that cannot be reached in nature.

Example: Flux qubit coupled to transmission line resonator

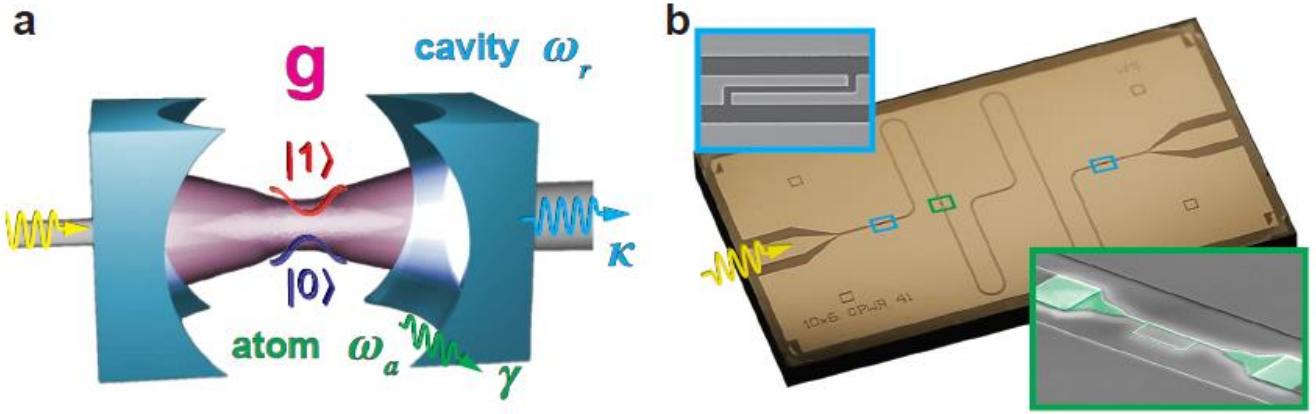


Figure 1.1: Analogies between cavity and circuit QED architectures. (a) Schematic of a cavity QED setup. The cavity (light blue) consists of two highly reflecting mirrors and supports the formation of a standing electromagnetic wave with fundamental resonance frequency ω_r. Mirror imperfections define a photon loss rate κ. An atom (green) with a transition frequency ω_a between the ground state $|0\rangle$ (blue) and the first excited state $|1\rangle$ (red) is placed inside the cavity. Spontaneous emission into modes other than the cavity mode is modeled by the atom decay rate γ. The atom-photon interaction rate g (magenta) depends on the atom's dipole moment and the electromagnetic field strength. (b) Photograph of a circuit QED setup as realized within this thesis. The cavity consists of a narrow, meandering strip of superconducting metal interrupted by small discontinuities (light blue box) acting analogue to the mirrors in the cavity QED setup. A superconducting flux qubit (green box) is fabricated at a suitable position and resembles an artificial atom. The decay rates κ and γ and the atom-photon interaction rate g are defined as in (a) but omitted in the picture for clarity.

IQM https://www.wmi.badw.de/publications/theses/Niemczyk_Doktorarbeit_2011.pdf

Generalized light-matter interaction: The quantum Rabi model

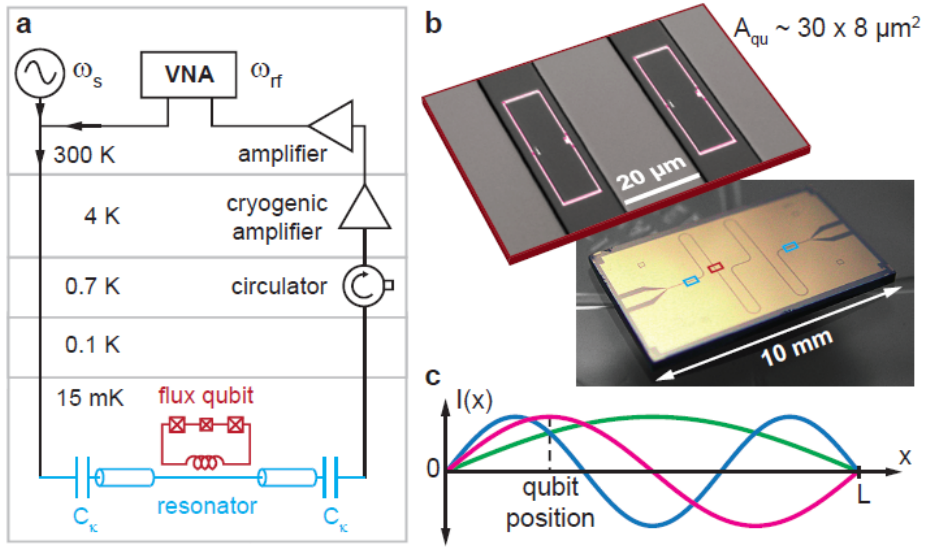


Figure 5.6: Measurement setup, images of the quantum circuit and sketch of the resonator's current distribution. (a) The amplified cavity transmission at ω_{rf} is probed using a vector network analyzer. For spectroscopy, a second tone ω_s can be applied to the cavity (light blue). For clarity, only one of the two qubits (dark red; crossed boxes represent Josephson junctions) is sketched. The microwave components are explained in the caption of Fig. 5.3. (b) Optical and false-color scanning electron images of the quantum circuit. The position of the flux qubits (magenta) is indicated by the red box and the light blue boxes mark the position of the coupling capacitors. (c) Sketch of the current distribution $I(x)$ of the first three resonator modes. Their resonance frequencies are: $\omega_1/2\pi = 2.624\,\mathrm{GHz}$ ($\lambda/2$-mode, green), $\omega_2/2\pi = 5.244\,\mathrm{GHz}$ (λ-mode, magenta) and $\omega_3/2\pi = 7.860\,\mathrm{GHz}$ ($3\lambda/2$-mode, blue). The cavity has a length $L = 23\,\mathrm{mm}$ and with $C_\kappa \sim 6\,\mathrm{fF}$, all quality factors $Q_n > 15 \cdot 10^3$.

We recall the following physical properties and their quantum mechanical description

Physical system / parameter	Effective Description
Qubit	$\mathcal{H}_q = \frac{\omega_q}{2}\hat{\sigma}_z\,.$
Resonator	$H = \hbar\omega_r\left(a^\dagger a + \frac{1}{2}\right)$
Magnetic field	$LI_{vac}(\hat{a} + \hat{a}^\dagger)$
Qubit energy bias	$\varepsilon(\hat{\sigma}_+ + \hat{\sigma}_-)$

If we bring qubit and resonator in close vicinity, we create a mutual inductance leading to a coupling term (interaction Hamiltonian)

$$\hbar g\left(\hat{\sigma}_+ + \hat{\sigma}_-\right)\left(\hat{a} + \hat{a}^\dagger\right)$$

Here, we are hiding all physical properties in the coupling constant g

IQM https://www.wmi.badw.de/publications/theses/Niemczyk_Doktorarbeit_2011.pdf

Generalized light-matter interaction: The quantum Rabi model

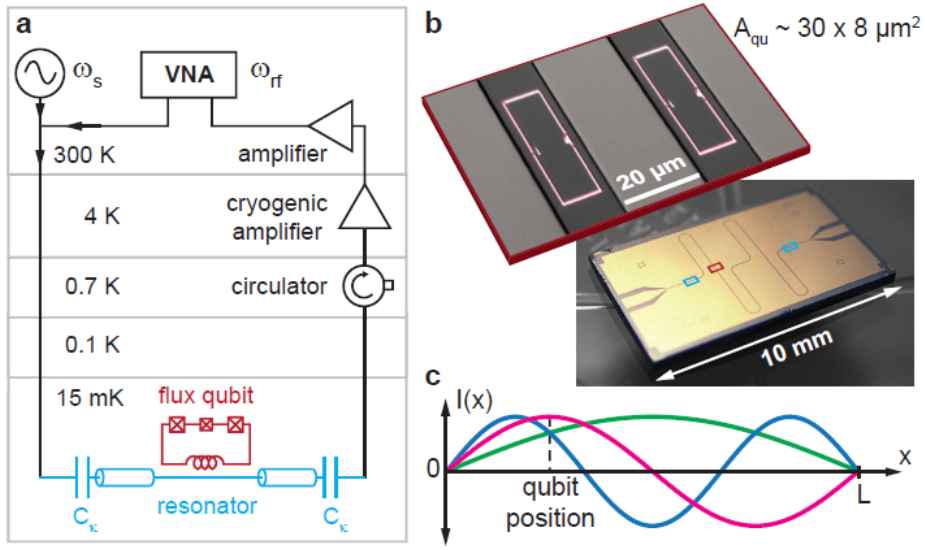
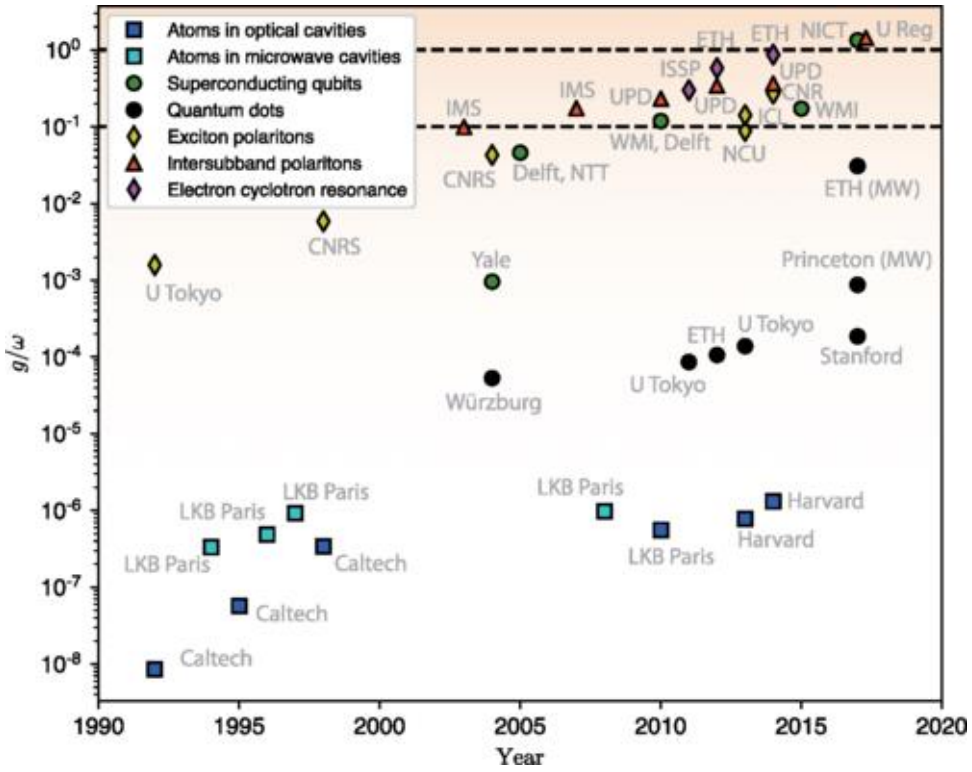


Figure 5.6: Measurement setup, images of the quantum circuit and sketch of the resonator's current distribution. (a) The amplified cavity transmission at ω_{rf} is probed using a vector network analyzer. For spectroscopy, a second tone ω_s can be applied to the cavity (light blue). For clarity, only one of the two qubits (dark red; crossed boxes represent Josephson junctions) is sketched. The microwave components are explained in the caption of Fig. 5.3. (b) Optical and false-color scanning electron images of the quantum circuit. The position of the flux qubits (magenta) is indicated by the red box and the light blue boxes mark the position of the coupling capacitors. (c) Sketch of the current distribution $I(x)$ of the first three resonator modes. Their resonance frequencies are: $\omega_1/2\pi = 2.624\,\mathrm{GHz}$ ($\lambda/2$-mode, green), $\omega_2/2\pi = 5.244\,\mathrm{GHz}$ (λ-mode, magenta) and $\omega_3/2\pi = 7.860\,\mathrm{GHz}$ ($3\lambda/2$-mode, blue). The cavity has a length $L = 23\,\mathrm{mm}$ and with $C_\kappa \sim 6\,\mathrm{fF}$, all quality factors $Q_n > 15 \cdot 10^3$.

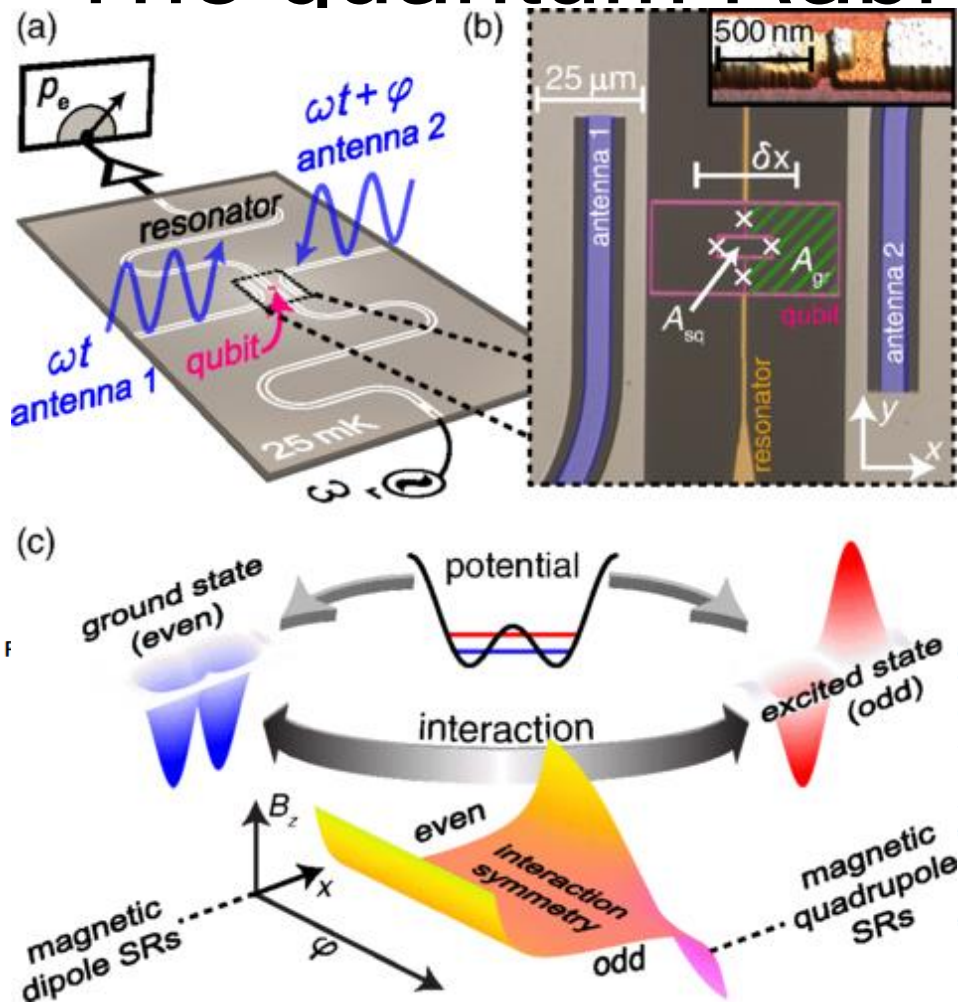
Adding the individual terms for qubit and resonator results in the system Hamiltonian

$$\mathcal{H}_{\mathrm{QR}} = \frac{\hbar\omega_{\mathrm{q}}}{2}\hat{\sigma}_z + \hbar\omega_{\mathrm{r}}\left(\hat{a}^\dagger\hat{a} + \frac{1}{2}\right) + \underbrace{\hbar g\left(\hat{\sigma}_+ + \hat{\sigma}_-\right)\left(\hat{a} + \hat{a}^\dagger\right)}_{\mathcal{H}_{\mathrm{int}}}$$

The above Hamiltonian is valid in all regimes for g

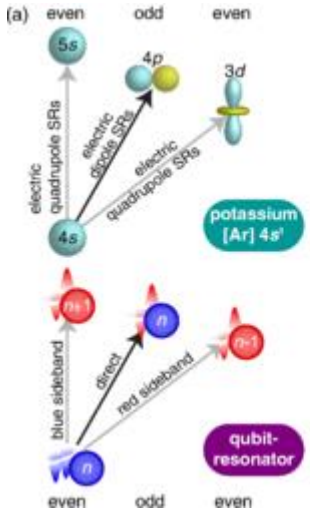


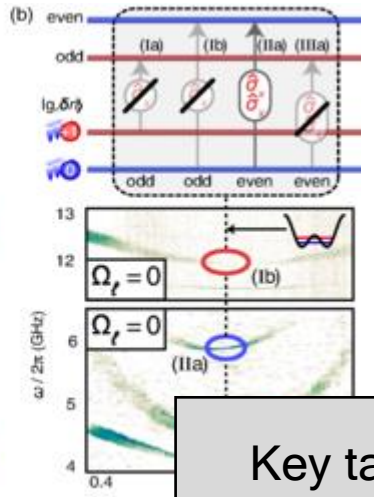
Generalized light-matter interaction: The quantum Rabi model



The counter rotating and counter intuitive terms $\hat{a}\,\hat{\sigma}_-$ and $\hat{\sigma}_+\hat{a}^\dagger$ give rise to the so-called Bloch-Siegert shift, which is hard to observe in nature but possible with superconducting systems.

The structure of the quantum Rabi Hamiltonian is such that the physical property “parity” is conserved. This is a special form of symmetry and one of the most fundamental concepts in physics.





The concept of parity for example gives rise to selection rules for allowed transitions in atoms. The same selection rules can be observed in superconducting circuits.

Key takeaway: Superconducting circuits follow the physics of quantum optics and can reach parameter regimes that are unreachable in nature.

https://journals.aps.org/prl/abstract/10.1103/PhysRevLett.121.060503

https://www.wmi.badw.de/publications/theses/Niemczyk_Doktorarbeit_2011.pdf

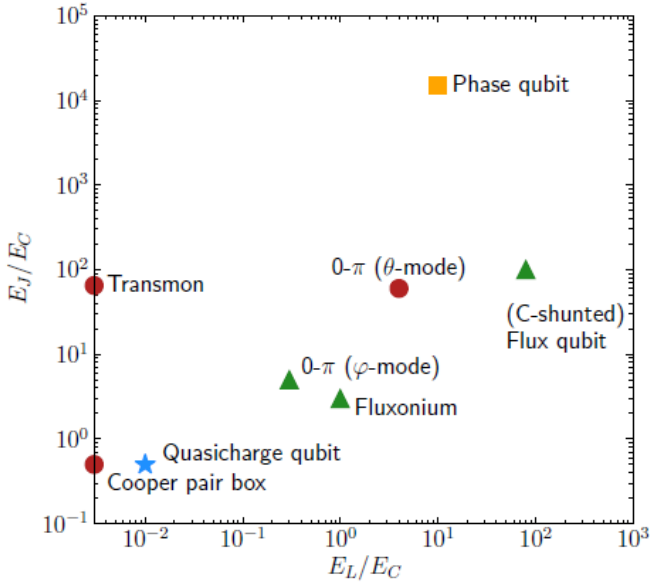
General note: Circuit QED

- Qubits can be seen as artificial atoms and resonators as microwave light.
- When we bring them close to each other we create “light-matter” coupling that is treated in the same way as quantum optics.
- Superconducting circuits allow on-chip study of quantum optics in regimes that cannot be reached in nature.

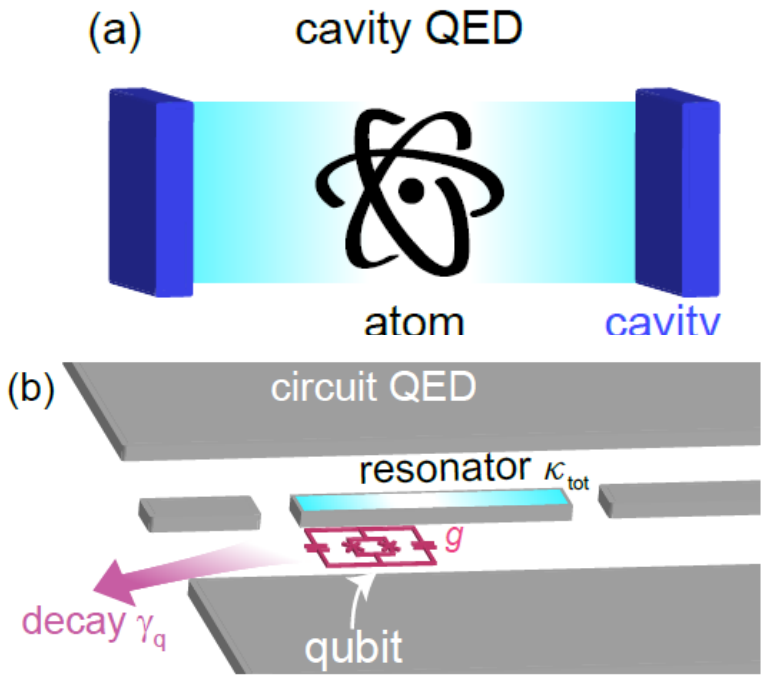
Agenda for today

8. Superconducting quantum circuits
   a. Qubits: Transmon qubit, Charge qubit, Flux qubit 1st DiVincenzo criteria
   b. Circuit-QED: Rabi model
   c. Rotating Wave approximation: Jaynes-Cummings model

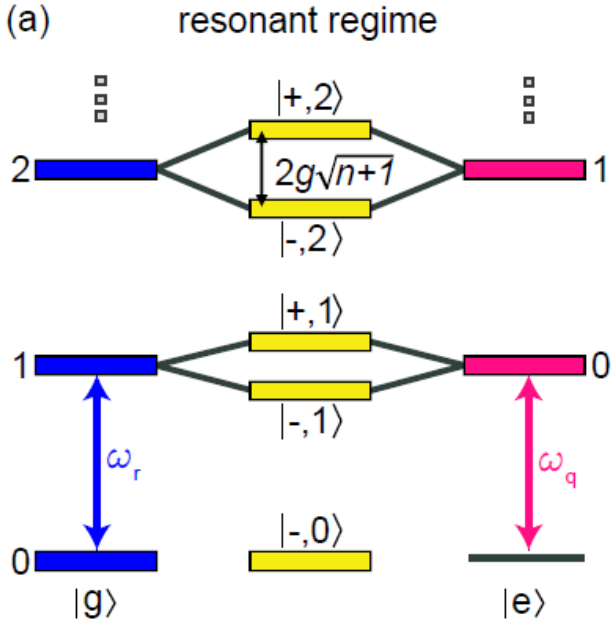
a.



b.



c.

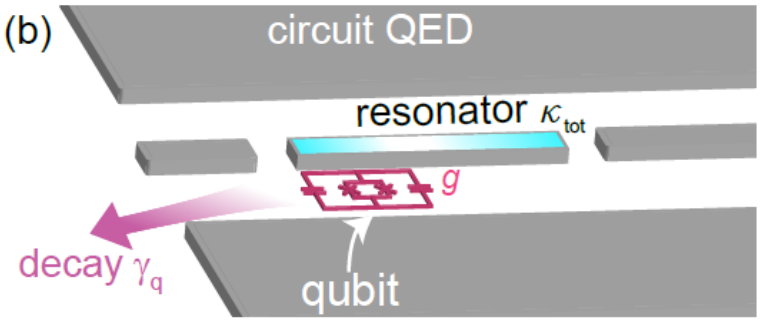


IQM

General note: Jaynes-Cummings model

- Usually one operates quantum circuits in a “practical” parameter regime, called strong coupling limit.
- In this limit, the coupling between qubit and electromagnetic field is much stronger as their loss rates but smaller than their eigenfrequencies.
- In this regime, the eigenstates experience a qubit state-dependent energy shift. Detecting this shift is used for qubit readout.

Rotating Wave approximation: Jaynes-Cummings model



We consider a transmon qubit that is capacitively coupled to a transmission line resonator. We operate in the strong coupling regime, where $g << \omega_q, \omega_r$.

This allows us to move into the interaction picture (a.k.a. rotating frame) defined as

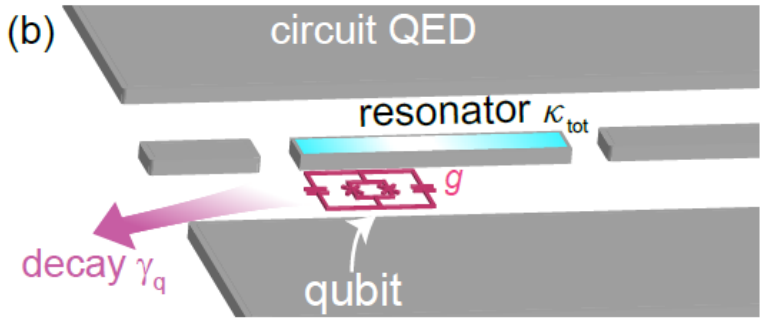
$$\hat{H}_{int}(t) = \frac{\hbar g}{2}\left(\hat{a}\hat{\sigma}_- e^{-i(\omega_r+\omega_q)t} + \hat{a}^\dagger\hat{\sigma}_+ e^{i(\omega_r+\omega_q)t} + \hat{a}\hat{\sigma}_+ e^{i(-\omega_r+\omega_q)t} + \hat{a}^\dagger\hat{\sigma}_- e^{-i(-\omega_r+\omega_q)t}\right).$$

This Hamiltonian contains both quickly and slowly oscillating components

$$\omega_r + \omega_q \qquad\qquad \omega_r - \omega_q$$

To get a solvable model, the quickly oscillating "counter-rotating" terms, are ignored. This is referred to as the rotating wave approximation, and it is valid since the fast oscillating term couples states of comparatively large energy difference.

Rotating Wave approximation: Jaynes-Cummings model



Transforming back into the Schrödinger picture the Jaynes-Cummings Hamiltonian is thus written as

$$\mathcal{H}_{\mathrm{JC}} = \frac{\hbar\omega_{\mathrm{q}}}{2}\hat{\sigma}_{\mathrm{z}} + \hbar\omega_{\mathrm{r}}\left(\hat{a}^{\dagger}\hat{a} + \frac{1}{2}\right) + \underbrace{\hbar g(\hat{\sigma}_{+}\hat{a} + \hat{\sigma}_{-}\hat{a}^{\dagger})}_{\mathcal{H}_{\mathrm{int}}} .$$

In the Jaynes-Cummings Hamiltonian, we can either excite the qubit by absorbing a photon $(\hat{\sigma}_{+}\hat{a})$ or take one excitation from the qubit and generate a photon $(\hat{\sigma}_{-}\hat{a}^{\dagger})$

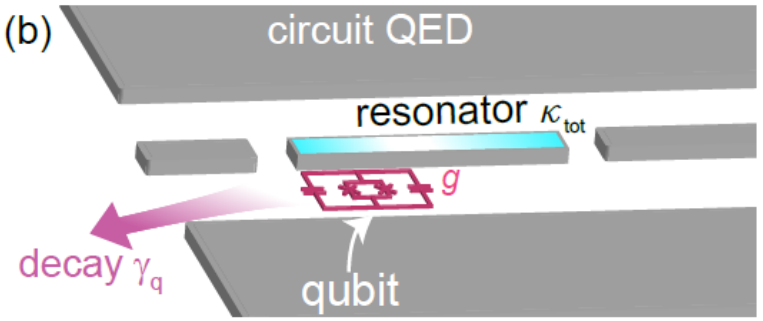
In the basis of uncoupled resonator excitation number (n_r) and qubit eigenstates, the Hamiltonian is transformed to

$$\mathcal{H}_{\mathrm{JC},n} = \frac{\hbar}{2}\begin{pmatrix} 2n_{\mathrm{r}}\omega_{\mathrm{r}} + \omega_{\mathrm{q}} & g\sqrt{n_{\mathrm{r}}+1} \\ g\sqrt{n_{\mathrm{r}}+1} & (n_{\mathrm{r}}+1)\omega_{\mathrm{r}} - \omega_{\mathrm{q}} \end{pmatrix} .$$

We can diagonalize this Hamiltonian and discuss two parameter regimes: Resonant, i.e. no detuning between qubit and resonator, and off-resonant, i.e. large detuning.

IQM https://mediatum.ub.tum.de/1326240

Rotating Wave approximation: Jaynes-Cummings model



The eigenfrequencies of the Jaynes-Cummings Hamiltonian are given as

$$\omega_{\pm,n} = (n_r + 1/2)\omega_r \pm 1/2\sqrt{\delta^2 + 4g^2(n_r + 1)}$$

Here, we have defined the detuning $\delta \equiv \omega_q - \omega_r$ and the ground state is $\omega_{-,0} = -\delta/2.$

The new dressed eigenstates of the system are the superposition states

$$|+,n_r\rangle = \cos\Theta_{n_r}\,|e,n_r\rangle + \sin\Theta_{n_r}\,|g,n_r\rangle$$

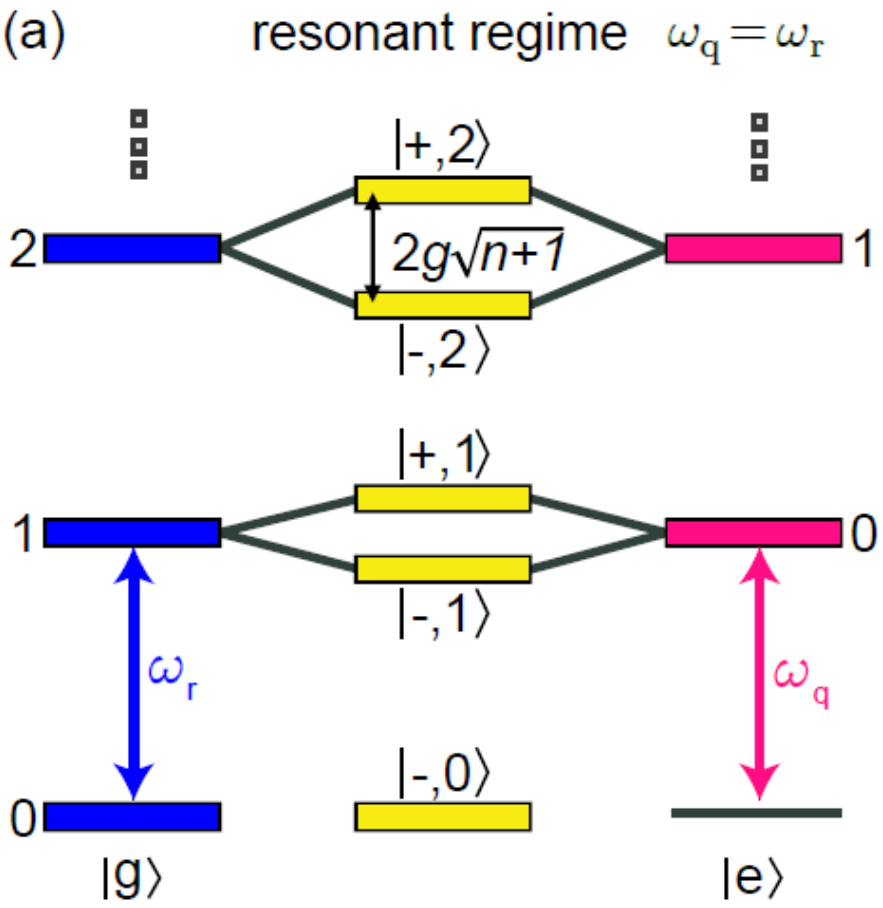
$$|-,n_r\rangle = \cos\Theta_{n_r}\,|g,n_r+1\rangle - \sin\Theta_{n_r}\,|e,n_r\rangle$$

Here, the mixing angle is a measure for the degree of entanglement between qubit and resonator states:

$$\Theta_n = \tan^{-1}(2g\sqrt{n_r+1}/\delta)/2$$

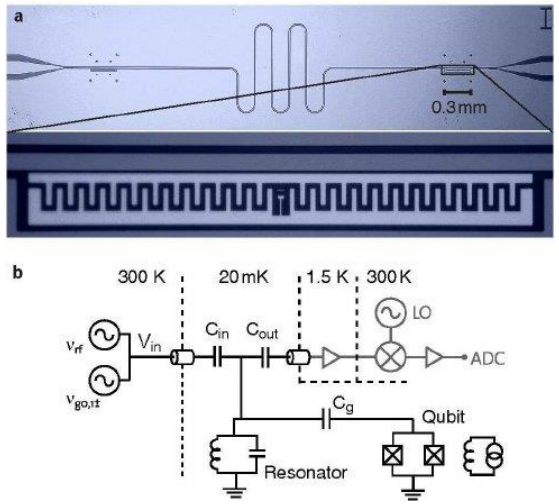
IQM https://mediatum.ub.tum.de/1326240

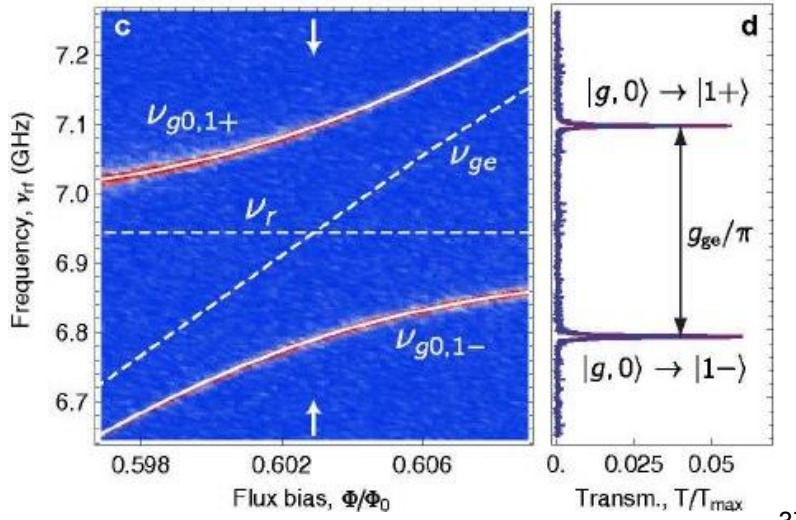
Rotating Wave approximation: Jaynes-Cummings model



When qubit and light mode are on resonance, i.e., $\delta \simeq 0$ the mixing angle $\Theta_n = \pi/4$is maximum and consequently there is strong entanglement.

In this regime, a coherent exchange of excitations between qubit and resonator occurs with the vacuum Rabi frequency $2g$. This interaction lifts the degeneracy of the corresponding eigenenergies By $2g\sqrt{n_r+1}$ to new doublet eigenstates.

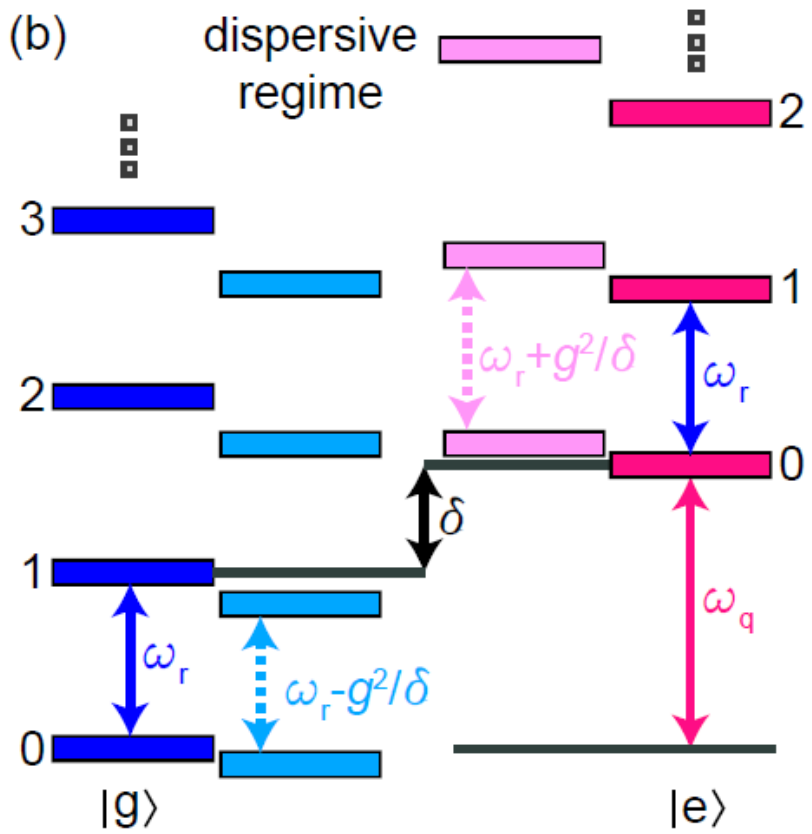




https://arxiv.org/abs/0902.1827

IQM https://mediatum.ub.tum.de/1326240

Rotating Wave approximation: Jaynes-Cummings model



In the dispersive regime, the detuning between qubit and resonator frequency is much larger than the coupling, i.e., $\delta \gg g$.

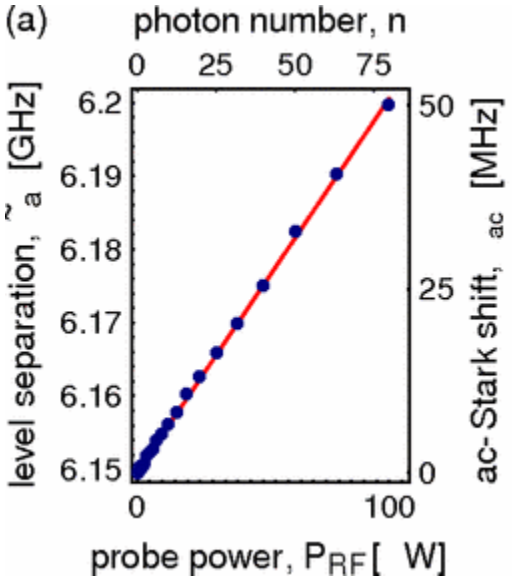
In this regime, there is no exchange of excitations anymore but virtual photons mediate a dispersive interaction between qubit and light field. This interaction leads to frequency shifts of the qubit and resonator eigenfrequencies. The dressed states are either more photon-like or more atom-like.

In the atom-like case (close to qubit states), the Hamiltonian can be derived as

$$\mathcal{H}_{\mathrm{disp}} \approx \hbar\omega_{\mathrm{r}}\left(\hat{a}^{\dagger}\hat{a} + 1/2\right) + \hbar/2\left(\omega_{\mathrm{q}} + 2\chi\hat{a}^{\dagger}\hat{a} + \chi\right)\hat{\sigma}_{\mathrm{z}}\,.$$

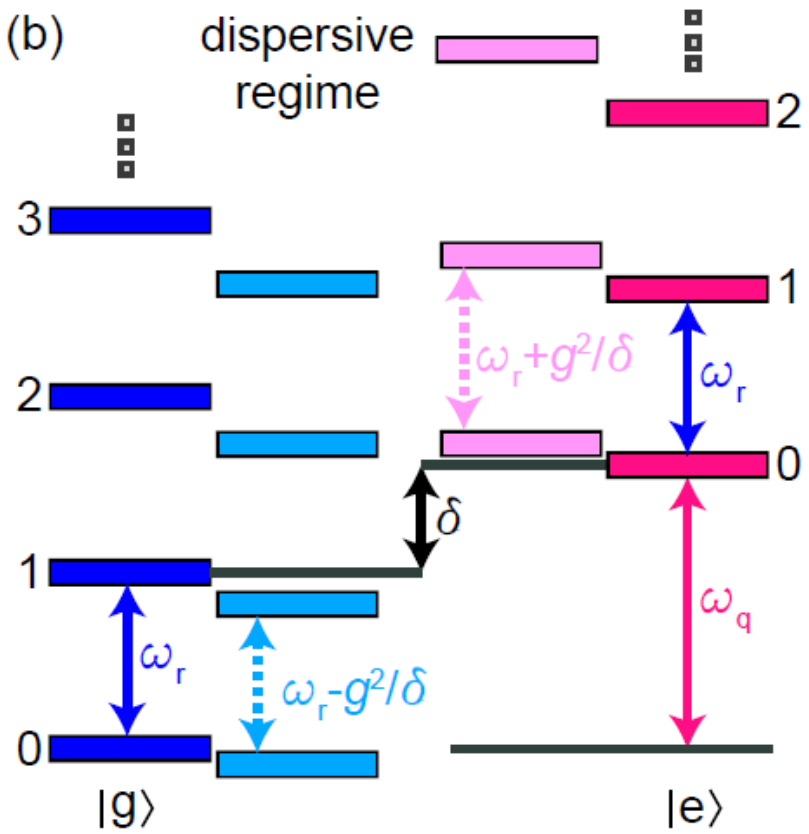
AC-Stark shift

Lamb shift



https://journals.aps.org/prl/abstract/10.1103/PhysRevLett.94.123602

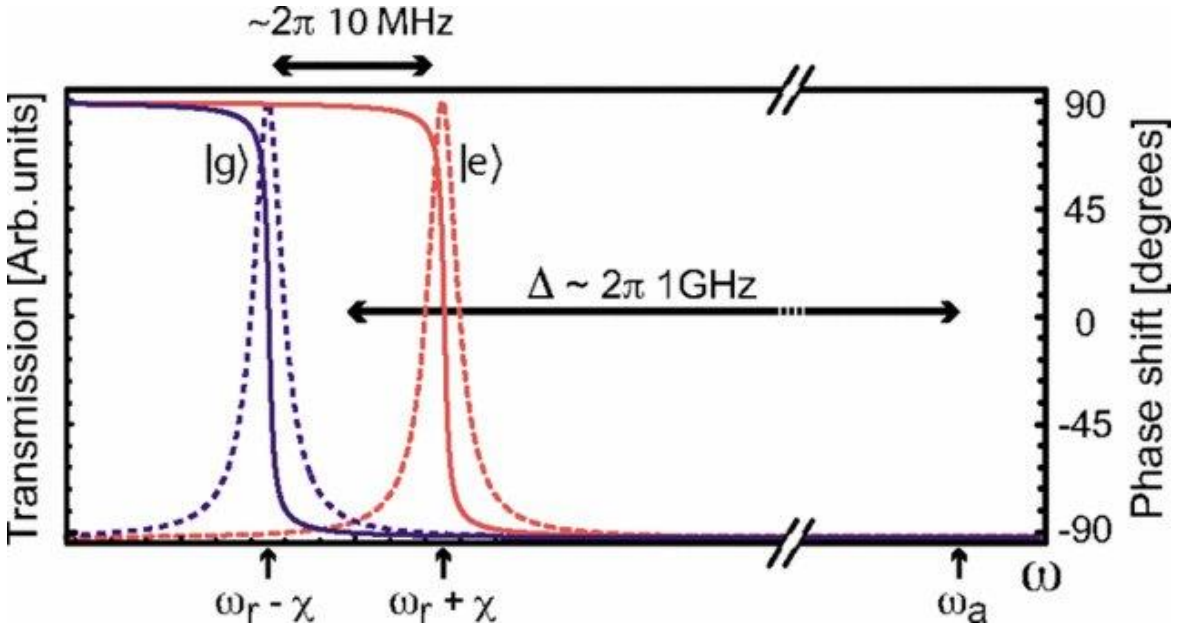
Rotating Wave approximation: Jaynes-Cummings model



In the photon-like case (close to resonator states), the Hamiltonian can be derived as

$$\mathcal{H}_{\mathrm{disp,r}} \approx \hbar\omega_{\mathrm{q}}\hat{\sigma}_{\mathrm{z}}/2 + \hbar\left(\omega_{\mathrm{r}} + \chi\hat{\sigma}_{\mathrm{z}}\right)\left(\hat{a}^{\dagger}\hat{a} + 1/2\right)$$

describing the qubit state-dependent resonator frequency, which we use for readout purposes.



https://journals.aps.org/pra/abstract/10.1103/PhysRevA.75.032329

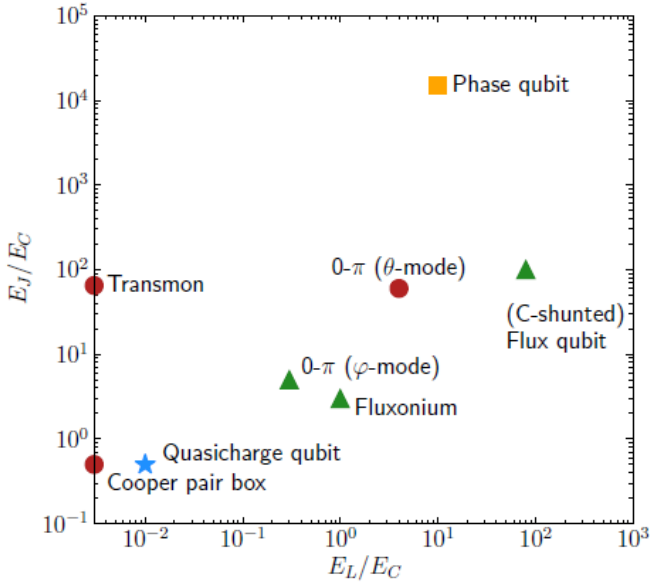
General note: Jaynes-Cummings model

- Usually one operates quantum circuits in a “practical” parameter regime, called strong coupling limit.
- In this limit, the coupling between qubit and electromagnetic field is much stronger as their loss rates but smaller than their eigenfrequencies.
- In this regime, the eigenstates experience a qubit state-dependent energy shift. Detecting this shift is used for qubit readout.

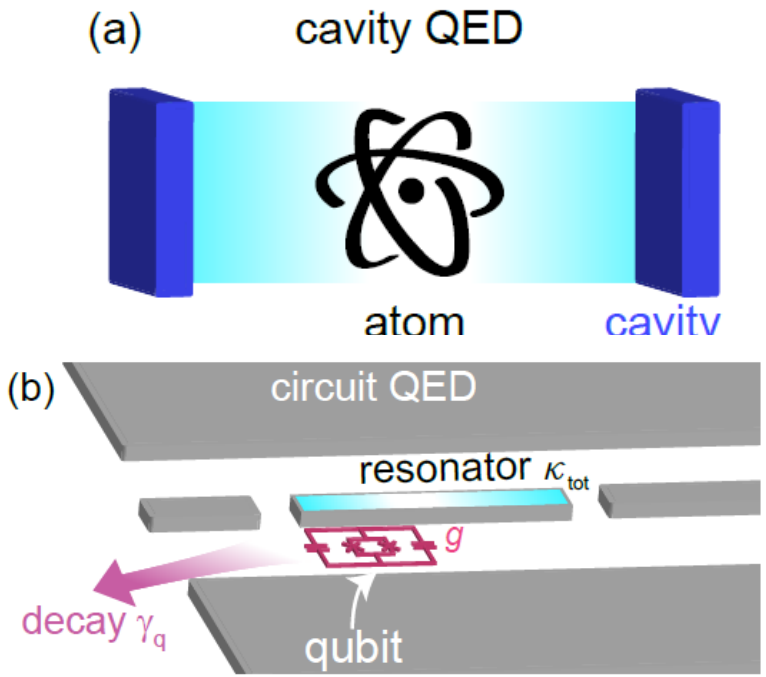
Agenda for today

8. Superconducting quantum circuits
   a. Qubits: Transmon qubit, Charge qubit, Flux qubit 1st DiVincenzo criteria
   b. Circuit-QED: Rabi model
   c. Rotating Wave approximation: Jaynes-Cummings model

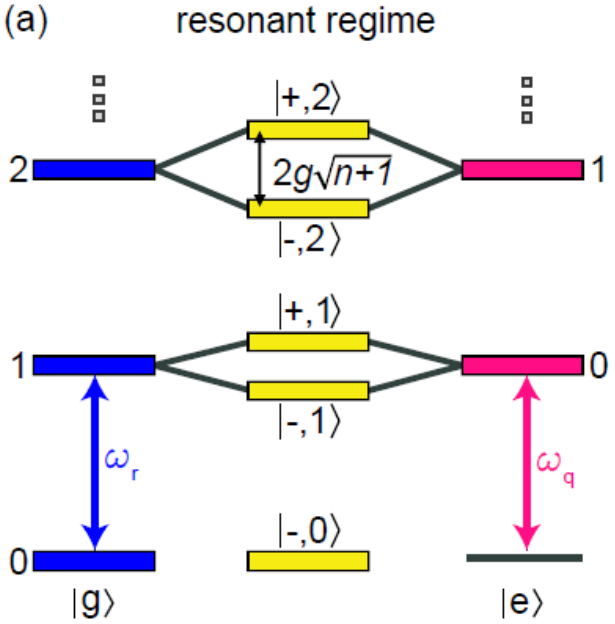
a.



b.



c.



IQM